Sofia Franco de Matos e Silva Neves

Bachelor's Degree in Biology

Unveiling the OsPIF15 and OsPIF16 regulatory network underlying rice coleoptile growth

Dissertation to obtain a Master's Degree in Biotechnology for Sustainability

Supervisor: Dr. Nelson Saibo, Principal Investigator, Head of the Plant Gene Regulation Lab (ITQB NOVA)

Co-supervisor: Dr. André Cordeiro, Researcher, Plant Gene Regulation Lab (ITQB NOVA)

September 2023

Sofia Franco de Matos e Silva Neves

Bachelor's Degree in Biology

Unveiling the OsPIF15 and OsPIF16 regulatory network underlying rice coleoptile growth

Dissertation to obtain a Master's Degree in Biotechnology for Sustainability

Supervisor: Dr. Nelson Saibo, Principal Investigator, Head of the Plant Gene Regulation Lab (ITQB NOVA)

Co-supervisor: Dr. André Cordeiro, Researcher, Plant Gene Regulation Lab (ITQB NOVA)

Jury:

President: Dr. Isabel Abreu (ITQB NOVA)

Opponent: Dr. Ana Confraria (ITQB NOVA)

ITQB NOVA

September 2023

UNVEILING THE OSPIF15 AND OSPIF16 REGULATORY NETWORK UNDERLYING RICE COLEOPTILE GROWTH

Acknowledgements

I would like to thank everyone who helped me grow in any way during this master's project.

To my supervisor, Dr. Nelson Saibo, for providing me with the opportunity to conduct my research and for the constant support and guidance throughout this entire project. Thank you for the incredible patience you showed towards all my stresses and anxieties and for the positive attitude and motivation whenever I doubted myself.

To my co-supervisor, Dr. André Cordeiro, whose invaluable expertise and insights were instrumental in helping shape my research and write this thesis. Thank you.

To Catarina, for your friendship and for all that you taught me during this time. Thank you for having my back since day one and for always being available to talk or to answer any of my questions. There is no one I would have rather spend all those long hours stressing about *calli* and yeast with.

To the rest of the PGR lab, for a good work environment and for the willingness to share their experiences and insights with me.

To everyone at GPlantS who welcomed me with open arms and helped me whenever I needed it.

To all my friends, for their love and support during this process, and a special thank you to Carol, for all your encouraging pep talks throughout the entire master's and for believing in me more than I did.

To my family, for their unconditional love and support during this project and always. Thank you to my incredible parents, for the financial and emotional support and for never giving up on me and always reaching out whenever I wasn't feeling my best. To my amazing siblings, and especially my sister, for all the emotional support hugs and cries when we were both feeling anxious.

To the rest of my family, thank you for your support and for always believing in my abilities.

Resumo

A luz é um estímulo ambiental fundamental para diversas fases de desenvolvimento e crescimento das plantas, incluindo o estabelecimento da plântula. Após emergência da plântula, os fotorrecetores de luz vermelha/vermelha-distante (fitocromos; phys) são foto-ativados e transladados para o núcleo, onde interagem com fatores de interação com fitocromos [PIFs; fatores de transcrição (TFs) bHLH], promovendo degradação dos PIFs ou inibindo a sua ligação a genes-alvo, e induzindo uma mudança de escoto- para fotomorfogénese. Em arroz, três fitocromos (OsphyA-C) e sete PIFs (OsPIF11-16, OsPIF8) foram identificados, mas esta rede regulatória permanece relativamente desconhecida. Quando crescemos mutantes *ospif* CRISPR/Cas9 com knock-out simples e duplo no escuro, os coleóptilos das plântulas *ospif15* e *ospif16* cresceram menos do que o tipo selvagem (WT), mas a diferença foi maior nas linhas *ospif15 ospif16*. Sob luz branca, vermelha e vermelha-distante, não houve diferenças significativas entre mutantes e WT. Assim, identificámos OsPIF15 e OsPIF16 como reguladores positivos da escotomorfogénese. Para entender melhor o papel funcional destes TFs na regulação do coleóptilo dependente da luz, investigámos as interações com OsphyA-C. Ambos os PIFs interagiram com OsphyB, mas apenas o OsPIF15 interagiu com OsphyA. Como TFs bHLH, a sua capacidade para homo- e heterodimerizar foi também testada, e resultados preliminares mostram que ambos OsPIF15 e OsPIF16 formam homo- e heterodímeros. A degradação de OsPIF15 mediada por OsphyB já foi descrita. Analisámos a estabilidade de OsPIF16 sob luz em WT e mutantes *phyB-1*, mostrando que a fotodegradação de OsPIF16 depende de OsphyB. Estes resultados sugerem que OsPIF15 e OsPIF16 são os principais reguladores positivos da escotomorfogénese, e a sua degradação após interação com Osphys promove fotomorfogénese. Concluindo, este estudo fornece novos conhecimentos acerca da função biológica dos OsPIFs na regulação do crescimento do coleóptilo pela luz e constitui uma excelente base para desvendar a regulação da foto- e escotomorfogénese em arroz.

Palavras-chave: fator de interação com fitocromos (PIF), alongamento do coleóptilo, escotomorfogénese, sinalização luminosa, arroz

Abstract

Light is a key environmental cue, influencing most stages of plant development and growth, including seedling establishment. Upon seedling emergence, red/far-red light-absorbing phytochromes (phys) are light-activated and translocated into the nucleus, where they interact with phytochrome-interacting factors [PIFs; bHLH transcription factors (TFs)], promoting PIF degradation or inhibiting PIFs from binding to their DNA targets, and shifting the seedling's developmental program from skoto- to photomorphogenesis. In rice, three phytochromes (OsphyA-C) and seven PIFs (OsPIF11-16, OsPIF8) have been identified, but this regulatory network remains fairly unknown. When CRISPR/Cas9 knockout single and double *ospif* mutants were grown under dark, *ospif15* and *ospif16* seedlings developed shorter coleoptiles than the wild-type (WT), but the difference was greater in the *ospif15 ospif16* lines. Under white, red and far-red light, there were no significant differences in coleoptile length between mutants and the WT. Thus, OsPIF15 and OsPIF16 were identified as positive regulators of skotomorphogenesis. To further uncover these TF's functional roles in light-dependent regulation of coleoptile growth, we investigated their interactions with OsphyA-C. Both OsPIFs interacted with OsphyB, but only OsPIF15 interacted with OsphyA. As members of the bHLH TF family, their ability to homo- and heterodimerize was tested as well, and preliminary results showed that both OsPIF15 and OsPIF16 form homo- and hetero-dimers. OsphyB-mediated degradation of OsPIF15 by light has already been described. We analyzed OsPIF16 stability under light in WT and *phyB-1* mutants and showed that OsPIF16 degradation by light is OsphyB-dependent. Our results suggest that OsPIF15 and OsPIF16 are key positive regulators of seedling skotomorphogenesis, and their degradation upon interaction with Osphys promotes photomorphogenesis. Overall, this work provides new insights into the biological function of OsPIFs in light regulation of rice coleoptile growth and is an excellent basis to further unveil the regulatory network underlying rice photo- and skotomorphogenesis.

Key words: phytochrome-interacting factor (PIF); coleoptile elongation; skotomorphogenesis; light signaling; rice

Table of contents

List of figures

List of tables

Abbreviations

°C Degrees Celsius

3-AT 3-Amino-1,2,4-triazole

AD GAL4 activation domain AD

Ade adenine

ANOVA analysis of variance

APA active phytochrome A-binding motif

APB active phytochrome B-binding motif

At *Arabidopsis thaliana*

BD GAL4 binding domain

bHLH basic Helix-Loop-Helix

BiFC Bimolecular Fluorescence Complementation

bp base pair

CCE cryptochrome C-terminal extension

CCML Co-Cultivation Medium Liquid

CCMS Co-Cultivation Medium Solid

cDNA complementary deoxyribonucleic acid

CDS coding sequence

ChIP-seq Chromatin Immunoprecipitation followed by sequencing

CIM Callus-Inducing Medium

cm centimeter

COP constitutive photomorphogenic

COP1 CONSTITUTIVELY PHOTOMORPHOGENIC1

CPF cryptochrome/photolyase family

CRISPR/Cas9 Clustered Regularly Interspaced Short Palindromic Repeats/CRISPR-associated protein 9

CRY-DASH cryptochrome-*Drosophila, Arabidopsis, Synechocystis*, human subclade

cv cultivar

Dc continuous darkness

ddH_2O double distilled water

DNA deoxyribonucleic acid

DTT dithiothreitol

ECL enhanced chemiluminescence

EDTA ethylenediamine tetraacetic acid

EIM Embryogenic Improvement Medium

ev empty vector

FAD flavin adenine dinucleotide

FHL fhy1-like

FHY1 far red elongated hypocotyl 1

FMN flavin mononucleotide

FR far-red

FR far-red light

FRc continuous far-red light

g gram

GAF Acronym derived from the first three protein families this domain was identified in (cyclic GMP (cGMP)-specific phosphodiesterases, adenylyl cyclases and FhlA)

h hour

HCl hydrochloric acid

HIR High Irradiance Response

His Histidine

HKRDs histidine kinase-related domains

HPTII hygromycin phosphotransferase II

***hpt*II** hygromycin resistance gene

HRP Horseradish Peroxidase

Hyg Hygromycin

InDels insertions and deletions

IP immunoprecipitation

kDa kilodalton

KO knock-out

L Liter

LAF laminar air flow

LB Luria-Bertani

Leu Leucine

LFR Low Fluence Response

LHC *LIGHT HARVESTING COMPLEX*

LiAc lithium acetate

LOV light oxygen voltage

m meter

mg milligram

min minute

mL milliliter

mM millimolar

ms millisecond

MSc Master of Science

MTHF methenyltetrahydrofolate

nm nanometer

O/N Overnight

OD_{600} optic density at 600 nm

Os Oryza sativa

ox overexpressing

PAS Per (period circadian protein), Arn (Ah receptor nuclear translocator protein), and Sim (single-minded protein).

PCR polymerase chain reaction

PDM Plantlet Development Medium

Pfr Phytochrome in the far-red-light-absorbing state

phy Phytochrome

PIF Phytochrome-Interacting Factor

PIL Phytochrome-Interacting Factor-Like

Pr Phytochrome in the red-light-absorbing state

PVDF polyvinylidene fluoride

R red

Rc continuous red light

RM Regeneration Medium

RNA-seq RNA sequencing

rpm revolutions per minute

RT Room Temperature

s second

SD Synthetic Defined

SDS Sodium Dodecyl Sulfate

SDS-PAGE Sodium Dodecyl Sulphate-Polyacrylamide Gel Electrophoresis

SgRNA Single-guide ribonucleic acid

SM Selection Medium

TF Transcription Factor

Trp Tryptophan

UV ultraviolet

UVR8 UV RESISTANCE LOCUS 8

V volt

VLFR Very Low Fluence Response

W White

Wc continuous white light

WT Wild-type

Y2H Yeast Two-Hybrid

YFP Yellow Fluorescent Protein

YPDA Yeast Peptone Dextrose Adenine

µg microgram

µL microliter

µM micromolar

µmol micromole

1. Introduction

1.1. Challenges to food security and the importance of rice as a staple food

In November 2022, global population reached 8 billion people (UN, 2022), and it is not expected to decline in the 21st century, with the United Nations (UN) projecting that it will likely grow to around 9.7 billion people by 2050 and 10.4 billion by 2100 (UN DESA, 2022). This rapid growth of the world population has not only generated unsustainable patterns of food production and consumption, but also contributed to both global warming and climate change, consequently leading to food insecurity and hindering the achievement of the Sustainable Development Goals (SGDs) set by the UN General Assembly for 2030 (FAO, 2016; Porter et al., 2014). Climate changes are reported to have reduced crop yield up to 70% since 1982, with only 3.5% of the global arable land area being safe from environmental limitations while food requirements continue increasing (FAO and IIASA, 2007; Raza et al., 2019). With agriculture playing a significant role in climate change and threatening biodiversity (Arora, 2019; Verchot et al., 2007), the intensification of agriculture and expansion of cultivated land to meet global food requirements is not a viable solution. The use of biotechnology, however, enables substantial alterations on crops to create cultivars with increased agricultural productivity and more capable of withstanding climate change. Thus, implementing the design of transgenic crops and sustainable agricultural practices using adequate policies is a crucial measure to attain food security while taking into consideration the ongoing climate changes (Munaweera et al., 2022). Being a staple food for more than half of the world's population, rice (*Oryza sativa* L.) can be a key player in providing food security and alleviating malnutrition (Gnanamanickam et al., 2002). However, with the decreasing availability of arable land, there is an urgent need to increase rice productivity as well as rice resistance to abiotic and biotic stresses, instead of increasing its cultivation. Therefore, understanding the mechanisms behind the regulation of desirable rice plant traits is essential to achieve high-yield cultivars capable of coping with the ever-changing environmental conditions.

1.2. Light as an environmental cue for plant growth and development

As sessile organisms, plants must cope with the ever-changing and often challenging environmental conditions that affect their growth and development, either at the cellular or morphological level. The key feature underlying plant survival under different environmental conditions lies on their plasticity, which is based on their ability to differentially express regulatory genes in response to both internal and external stimuli (Schlichting, 1986). Thus, plants have evolved sophisticated regulatory networks to perceive and interpret environmental cues and mediate responses towards optimal growth and development. Among these signals, light is one of the most important throughout the entire life cycle, influencing numerous aspects of plant development, from germination to reproductive development (Singh et al., 2015). The effect of red (R):far-red (FR) light ratio on germination, has long been known. For instance, in lettuce, it was shown that far-red light inhibits germination of light-sensitive seeds while red light promotes it (Flint & McAlister, 1935, 1937). Once germination is complete, the young seedling's establishment is conditioned by various factors, such as soil pH, drought (Sadeghian & Yavari, 2004),

planting depth, temperature (Stevens et al., 2014), salinity (Uçarlı, 2020) and light (Singh et al., 2015). Depending on light availability, seedling development, which is a crucial and highly susceptible stage of plants' life cycles and a major determinant of plant yield and food security (Finch-Savage & Bassel, 2016), is carried out through two distinct pathways. Below the soil and in the absence of light, the heterotrophic seedlings undergo skotomorphogenesis, which is characterized, in the model species *Arabidopsis thaliana*, by the development of an etiolated hypocotyl and an apical hook to the detriment of cotyledon and root development, in an effort to economize seed resources. Once the seedling reaches the surface in pursue of light, it adopts an autotrophic growth strategy, known as photomorphogenesis. In Arabidopsis, this process is characterized by an attenuated hypocotyl growth rate, opening of the apical hook and cotyledon expansion and greening due to chlorophyll biosynthesis (Chory, 1993; Fankhauser & Chory, 1997; Gommers & Monte, 2018; Josse & Halliday, 2008). Seedling survival depends on the ability of plants to properly conduct light signal transduction. Although the complete signaling cascade is yet to be described, plant photoreceptors have been identified as key players in this process (Josse & Halliday, 2008).

1.3. Photoreceptors in plants

Land plants are constantly perceiving changes in their surrounding environment and modulating their growth and development according to such changes. One of the most important environmental cues modulating plant growth is light, which can vary in terms of quality, quantity, direction, and photoperiod. These signals are perceived by photoreceptors that transduce them via sophisticated signaling cascades to ultimately regulate the transcription of light-regulated genes, thus ensuring suitable physiological and developmental responses (Jiao et al., 2007; Kami et al., 2010). Since green light is reflected by green plants, most of the research regarding light-mediated plant development has been directed towards understanding the mechanisms behind the responses to ultraviolet (UV), blue, red and far-red wavelengths and characterizing the photoreceptors that respond specifically to these regions of the light spectrum (Battle et al., 2020; Johkan et al., 2012). To date, three major photoreceptor families have been identified and characterized in *Arabidopsis thaliana*. Phytochromes perceive light in the red/far-red regions of the spectrum (600-750 nm), while blue/UV-A wavelengths (320–500 nm) are perceived by cryptochromes and phototropins (Sullivan & Deng, 2003; H. Wang, 2005). Additionally, the UV RESISTANCE LOCUS 8 (UVR8) was more recently identified as a UV-B (280–315 nm) light photoreceptor (Rizzini et al., 2011).

1.3.1. Cryptochromes

Cryptochromes, which act as UV-A/blue light receptors, possess two domains: the N-terminal PHR (Photolyase-Homologous Region) domain, which is the chromophore-binding domain capable of light absorption, and the C-terminal CCE (Cryptochrome C-terminal Extension) domain, which does not directly participate in blue light perception but is involved in blue light-induced protein-protein interactions

(Lin & Shalitin, 2003; Ponnu & Hoecker, 2022). In Arabidopsis, CRY1 and CRY2 have been well-characterized as photoreceptors belonging to the cryptochrome/photolyase family (CPF) of flavoproteins, whereas CRY3 belongs to the cryptochrome-*Drosophila, Arabidopsis, Synechocystis*, human (CRY-DASH) subclade of the CPF (Kiontke et al., 2020). The PHR domain sequences of Arabidopsis CRY1 and CRY2 share homology with that of DNA photolyases, but the blue/UV-A light-dependent DNA repairing activity found in these flavoenzymes has not been reported in the cryptochromes at issue (Sancar, 2003). On the contrary, CRY3 has been found to be involved in DNA repair, although its function as a photoreceptor remains unclear (Pokorny et al., 2008). The chromophores of cryptochromes consist of a primary catalytic flavin adenine dinucleotide (FAD) and a secondary deazaflavin or pterin (methenyltetrahydrofolate; MTHF) that acts as a light-harvesting antenna pigment (Sancar, 2003; H. Wang, 2005). It has been shown that, upon irradiation with blue light, cryptochromes undergo photoactivation. As MTHF is excited by photon absorption, the excitation energy is transferred to the ground state oxidized FAD, semi-reducing it to the $FADH^{\bullet}$ neutral radical and inducing the dissociation of the PHR and CCE domains with subsequent transduction into a signaling cascade required for the response to cryptochrome activation (Bouly et al., 2007; Q. Wang & Lin, 2020). The adaptation of an open conformation by the photoexcited cryptochrome allows it to undergo autophosphorylation and dimerization, triggering ubiquitination-dependent protein degradation and consequently altering interactions between the photoreceptor and its signaling partners, affecting gene expression and plant development (Sang et al., 2005; Shalitin et al., 2002, 2003). Even though Arabidopsis CRY1 and CRY2 are both nuclear proteins, CRY2 seems to be constitutively imported to the nucleus regardless of light conditions (Yu et al., 2007), while CRY1 can be exported or remain in the cytosol under light exposure but is imported into the nucleus in the dark (G. Wu & Spalding, 2007). CRY3 likely acts in the mitochondria and chloroplasts (Kleine et al., 2003). The functions of Arabidopsis cryptochromes and phytochromes in the regulation of photomorphogenic development seem to almost fully overlap, with both photoreceptors mediating de-etiolation, gene expression, and photoperiodic flowering, in response to blue/UV-A and red/far-red light, respectively. Arabidopsis cry1 and cry2 have been reported to mediate possibly all blue light-dependent de-etiolation responses (Lin, 2002), such as inhibition of hypocotyl elongation (Lin et al., 1998; Young et al., 1992). Additionally, the activation of floral transition by cry1 (Exner et al., 2010) and the involvement of cry2 in the photoperiodic regulation of flowering time (Guo et al., 1998) have also been described in studies using cryptochrome mutants, and both cryptochromes are reported to regulate the period length of the circadian clock (Somers et al., 1998). Moreover, mutation or overexpression of cry1 and/or cry2 has been shown to affect blue light regulation of gene expression in several Arabidopsis genes (L. Ma et al., 2001). While the function of rice cryptochromes is not as well understood, inhibition of coleoptile elongation upon blue light irradiation has been demonstrated in rice transgenic lines overexpressing the *OsCRY1a* or *OsCRY1b* gene, compared to the WT, suggesting that these two proteins are involved in blue light-mediated inhibition of rice coleoptile elongation. Additionally, late flowering in *OsCRY2* antisense transgenic rice plants compared to WT under long- and short-day conditions suggests that Oscry2 promotes flowering time in rice (Hirose et al., 2006).

1.3.2.Phototropins

Phototropins are UV-A/blue light photoreceptors that possess a C-terminal serine-threonine kinase domain and a photosensory domain at the N-terminus comprised of two light oxygen voltage (LOV) domains with an associated flavin mononucleotide (FMN) as a chromophore responsible for light absorption (Kagawa, 2003). Upon blue light irradiation, the binding of the FMN to each LOV domain induces a conformational change in the protein, producing the active LOV_{390} species, which absorbs maximally at 390 nm. Under darkness, this change can be rapidly reversed to the inactive LOV_{447} state (Christie, 2007; Demarsy & Fankhauser, 2009). While phytochromes and cryptochromes are key players in photomorphogenesis, phototropins, which can cycle between the active and inactive state depending on the light conditions, are involved in light-dependent processes thought to optimize photosynthesis and plant growth. The two phototropins found in Arabidopsis (phot1 and phot2, previously designated as NPH1 and NPL1) play partially overlapping roles in the regulation of hypocotyl phototropism and chloroplast relocation (Sakai et al., 2001; Wada et al., 2003), and act redundantly in the control of stomatal opening (Kinoshita et al., 2001) and leaf expansion (Sakamoto & Briggs, 2002). In rice, two *PHOT1* homologues (*PHOT1* and *PHOT2* previously designated as *OsNPH1a* and *OsNPH1b*) have been isolated and characterized and their expression was found to be differentially regulated by light in different rice seedling tissues. PHOT1 was found to be predominant in the coleoptile and downregulated by light, whereas PHOT2 is more abundant in leaves and is upregulated by light (Kanegae et al., 2000).

1.3.3.UVR8

UVR8 is a UV-B specific photoreceptor whose monomer structure consists of a seven-bladed β-propeller protein. Purified UVR8 occurs as a homodimer which, upon UV-B light exposure, dissociates into monomers. Monomerization ergo allows the interaction with the E3 ubiquitin ligase CONSTITUTIVELY PHOTOMORPHOGENIC1 (COP1), triggering a signaling cascade that mediates UV-B-induced photomorphogenic responses (Rizzini et al., 2011). Unlike the afore-mentioned photoreceptors, the UVR8 from *A. thaliana* does not employ a bound prosthetic chromophore to absorb light. Instead, photoreception of UV-B light is attained through intrinsic tryptophan (Trp) residues at the dimer interaction surface (Christie et al., 2012). Even though these residues have been identified, the molecular mechanism that links UV-B photoreception to UVR8 monomerization and the mechanism of action of COP1 in UV-B response remain unclear (Jenkins, 2014). Although a comprehensive phylogenetic analysis of UVR8 proteins has demonstrated their functional conservation from green algae to higher plants (Fernández et al., 2016), little advancement has been made in regards to understanding the mechanisms behind the ability of different crop species to respond to UV-B light. Recently, ZmUVR8, the maize homologue of UVR8 was shown to function as a UV-B photoreceptor in Arabidopsis (Fernández et al., 2020). Rice has two *UVR8* homologues, identified as *OsUVR8a* and *OsUVR8b*. In an effort to establish rice as a model plant for UV-B signaling studies, Idris and collegues, 2020 investigated the UV-B-induced responses of rice seedlings of a Tos17 insertion line of *OsUVR8a* and found that the shoots of seedlings grown in white light showed no expression of *OsUVR8a*, but

normal expression of *OsUVR8b*, exhibiting UV-B-induced inhibition of coleoptile growth. They have yet to confirm if these UVR8 homologs function as the UV-B photoreceptor in rice.

1.3.4. Phytochromes

1.3.4.1. Phytochrome structure and intracellular localization

Phytochromes (phys) are photoreceptors whose main photosensory function is to perceive variations in the red:far-red (R:FR) light ratio in the natural light environment (Smith, 1982). *In vivo*, phytochromes exist as homo- or heterodimeric chromoproteins (Sharrock & Clack, 2004). They are composed of two soluble polypeptides of ~125 kDa, each covalently attached to a linear tetrapyrrole chromophore (phytochromobilin), whose photochemical activity allows phys to interconvert between the physiologically inactive red light-absorbing form (Pr) and the active far-red light-absorbing form (Pfr) (Bae & Choi, 2008; Fankhauser & Chory, 1997). Each polypeptide contains a highly conserved photosensory N-terminal domain and a regulatory C-terminal domain involved in dimerization and downstream signaling (Jones & Edgerton, 1994; Quail et al., 1995). The N-terminal of plant phytochromes is further divided into four domains named P1, P2 or Per-Arnt-Sim (PAS) domain, P3 or cGMP phosphodiesterase/adenylyl cyclase/FhlA (GAF) domain, and P4 or PHY domain, while the C-terminal encompasses two PAS-related domains (PRDs) and two histidine kinase-related domains (HKRDs) (Kay, 1997; Lagarias et al., 1995; S. Wu & Lagarias, 2000). Evidence shows that, in the dark, *de novo* synthesized phytochromes in the Pr form are cytosolically localized and undergo nucleocytoplasmic partitioning upon conversion to the Pfr form due to light irradiation, and further compartmentalization to subnuclear structures known as photobodies (Yamaguchi et al., 1999). Because of the high R:FR ratio in sunlight, Pfr is the predominant form of phytochromes inside the cells of light-grown seedlings but it can be converted back to the Pr form upon far-red light absorption (photoconversion) or through spontaneous thermal relaxation (dark or thermal reversion) (Kircher et al., 1999; Sakamoto & Nagatani, 1996; Schäfer & Bowler, 2002; Yamaguchi et al., 1999).

1.3.4.2. Phytochrome light-regulation and function

The phytochrome apoproteins of angiosperms are encoded by a small nuclear gene family which, in Arabidopsis, comprises five members, denoted *PHYA-PHYE*, while monocots, such as rice, lack the orthologs of *PHYD* and *PHYE* of Arabidopsis, but possess homologues of *PHYA*, *PHYB* and *PHYC* (Clack et al., 1994; Mathews & Sharrock, 1996). Studies using phytochrome-deficient mutants of Arabidopsis, have enabled researchers to elucidate the distinct and overlapping modes of action of each phytochrome in mediating plant photoresponses in this model (Quail, 1998; G. C. Whitelam & Devlin, 1997). Upon light irradiation, different types of photoresponses can be triggered, depending on the wavelength and light fluence rate required to trigger them: Very Low Fluence Response (VLFR) occurs under FR light pulses (≈10^{-1} to 10 μmol m^{-2} intensity) or very low fluences of pulsed of continuous R light (≈10^{-4} to 10^{-1} μmol m^{-2} intensity); Low Fluence Response (LFR) is observed under continuous or pulsed R light (≈10 μmol m^{-2} or higher intensity); and High Irradiance Response (HIR) takes place under

continuous R (R-HIR) or FR (FR-HIR) light (≈1 μmol m^{-2} s^{-1} or greater fluence rate) (Mohr, 1962; Sheerin & Hiltbrunner, 2017; Sineshchekov, 2023). Depending on their light lability, phytochromes can be divided into two groups: the type I phytochrome (phyA) is unstable under light in the Pfr form, making it much more abundant in etiolated seedlings than in light-grown ones, whereas type II phytochromes (phyB-phyE) are present at similar constitutive levels in both dark- and light-grown seedlings due to their higher stability in the Pr form (Fankhauser & Chory, 1997).

While the precise mechanism behind light-induced phytochrome signaling remains elusive, various studies have unraveled the central role of basic Helix-Loop-Helix (bHLH) transcription factors, such as Phytochrome-Interacting Factors (PIFs), through their physical interaction with phytochromes (reviewed in Pham et al., 2018). Under darkness, the inactive Pr is cytosolically localized, enabling PIFs to accumulate in the nucleus and negatively regulate light responses by repressing photomorphogenesis and promoting the skotomorphogenic phenotype. Studies in Arabidopsis have shown that, in LFR, upon R light exposure, the Pr form of phyB suffers a conformational change that exposes its nuclear localization signal, leading to its rapid translocation from the cytosol to the nucleus in the Pfr form. Once in the nucleus, the biologically active Pfr physically interacts with PIFs, leading to PIF phosphorylation, ubiquitination and 26S proteasome-dependent degradation or inhibiting them from binding to and activating their DNA targets. This induces a transcriptional cascade that leads to the expression of light-responsive genes, ultimately resulting in photomorphogenic development (Butler et al., 1959; Favero, 2020). After exposure to FR light, Pfr is then converted back to the Pr form. This reversibility, however, is not observed in phyA-mediated FR-HIR and VLFR and phyB-mediated R-HIR (Sheerin & Hiltbrunner, 2017). The lack of de-etiolation responses in etiolated Arabidopsis *phyA* mutant seedlings grown under prolonged FR light irradiation, but not under prolonged R light irradiation, suggests that phyA mediates FR-HIR but not R-HIR (Nagatani et al., 1993; Parks & Quail, 1993; Garry C. Whitelam et al., 1993). Furthermore, when exposed to R or FR light pulses, the seeds of *phyA* Arabidopsis mutants show no VLFR but strong LFR, respectively, indicating that phyA must also be involved in the VLFR signaling mode (Botto et al., 1996; Shinomura et al., 1996). In contrast, phyB controls the LFR in R light-dependent germination (Shinomura et al., 1996).

The production and characterization of rice phytochrome knockout mutants has allowed for advances in understanding how rice plants react to different light conditions through phytochromes. It has been reported that phyB is a key player in coleoptile growth inhibition under Rc, but not under FRc and that phyA also plays an important role in coleoptile inhibition under Rc, but only in the absence of phyB (Takano et al., 2005). Additionally, both phyA and phyC are capable of FRc light perception, with phyC's function being non-essential when phyA is functional. When WT and *phyA*-1 mutants were grown under Dc and Rc light, both exhibited typical coleoptile elongation and coleoptile growth inhibition, respectively. Under FRc light, only the WT exhibited shorter coleoptiles, with the coleoptiles of *phyA*-1 mutants being similar to those of dark-grown seedlings, suggesting that rice phyA is the dominant photoreceptor of FRc light (Takano et al., 2001). The *phyb* mutation does not affect coleoptile inhibition under FRc. So, FR light can affect coleoptile elongation by either activating phyA or inactivating phyB (Takano et al., 2001, 2005).

1.4. Phytochrome-interacting factors in Arabidopsis and rice

In Arabidopsis, the bHLH protein class is comprised of more than 150 putative transcription factors, 15 of which are involved in light signaling, making up the PIF subfamily of transcription factors. Of these proteins, 8 members, denominated PIF1, PIF2 - which was previously denominated PHYTOCHROME INTERACTING FACTOR3-LIKE1 (PIL1) - and PIF3-PIF8, have been reported to preferentially interact, *in vitro*, with the Pfr form of phytochromes via a conserved active phytochrome-binding motif located in their N-terminal domain (Khanna et al., 2004). While all Arabidopsis PIFs contain the active phytochrome B-binding (APB) motif, only PIF1 and PIF3 possess the additional active phytochrome A-binding (APA) motif, with PIF1 showing stronger affinity for phyA than PIF3 (Huq et al., 2004; Lee & Choi, 2017). PIF3 was the first bHLH protein identified as a phytochrome-interacting factor, when it was shown to directly interact with the C-terminal domains of both AtphyA and AtphyB. When independent transgenic Arabidopsis lines expressing either sense or antisense *PIF3* cDNA sequences were grown under R and FR light, their development was affected compared to the WT, but, under dark, no differences were observed. This result showed that PIF3 regulates light-dependent seedling development via physical interaction with phA and phyB (Ni et al., 1998).. Moreover, because *PIF4*-antisense lines show similar hypocotyl length compared to the WT under FRc, and PIF4 has little affinity for phyA, it was suggested that PIF4 may be specific to phyB signaling (Huq & Quail, 2002). PIF5 and PIF4 are selectively degraded upon interaction with R light-activated phyB, but remain present at high levels under low R:FR ratios, promoting hypocotyl elongation in the shade-avoidance response (Lorrain et al., 2008), with PIF7 also collaborating in this response in a synergistic manner (Leivar, Monte, Al-Sady, et al., 2008; L. Li et al., 2012). In a study where a loss-of-function mutant of PIF6 (*pif6-1*), transgenic lines overexpressing PIF6 (PIF6-ox), and WT were grown under Rc light, *pif6-1* seedlings displayed shorter hypocotyls than the WT and PIF6-ox seedlings displayed a reverse phenotype similar to that of *phyB* mutant seedlings, but these morphological differences were far less evident when the plants were grown under FRc, suggesting that PIF6 acts as a negative regulator of phyB in the red-light signaling pathway that regulates the photomorphogenic response during seedling de-etiolation (Fujimori et al., 2004). PIF8 differs from other PIFs in its protein accumulation pattern, being more highly accumulated under FR than under R light or darkness, and in its functional roles under different light conditions, seeing as it inhibits phyA-induced suppression of hypocotyl elongation, but does not inhibit phyB-induced R light response (J. Oh et al., 2020).

The rice genome contains 167 genes that encode putative bHLH proteins (X. Li et al., 2006) and, to date, seven have been identified as PIFs. Initially, a set of highly conserved orthologs of AtPIFs were identified as OsPIL11-16 (henceforth designated as OsPIF11-16), sharing, not only a highly conserved bHLH DNA-binding domain, but also the crucial active phytochrome-binding motif at their N-terminal, with PIF3. In this same study, OsPIF13 was suggested to be a functional counterpart of PIF6. OsPIF15 and OsPIF16, whose expression during de-etiolation in response to light was repressed (Yamashino et al., 2003), appeared to be orthologs of PIF3 (Nakamura et al., 2007a). More recently, a PIF8 homolog (OsPIF8) that possesses a bHLH motif and an APB motif, but no APA motif, was identified as the seventh rice PIF (J. Oh et al., 2020). Of these OsPIFs, only OsPIF14-16 have been found to interact with phyB (Cordeiro et al., 2022), and OsPIF13 was found to not interact with this phytochrome, despite

possessing an APB motif (Todaka et al., 2012). OsPIF15 and OsPIF16 are the only OsPIFs that possess an APA motif, but their interaction with OsphyA is yet to be tested (Cordeiro et al., 2022).

1.4.1. Gene network regulating seedling skotomorphogenesis

Under dark, Arabidopsis seedlings adopt a skotomorphogenenic developmental program, in which seed reserves are preferentially allocated toward hypocotyl elongation while cotyledon and root development are sacrificed, until the seedling becomes photosynthetically competent and autotrophic. In monocots, seedlings typically undergo coleoptile elongation under dark to protect the first true leaf (Gommers & Monte, 2018). Genetic screenings for Arabidopsis mutants that exhibit de-etiolated (DET) or constitutive photomorphogenic (COP) phenotypes under dark have allowed a deeper understanding of photomorphogenesis repression under dark. From these screenings, photomorphogenesis repressors, involved in ubiquitin-proteasome-mediated protein degradation, such as COP1, COP10 and SPA1-4, have been identified (Chen & Chory, 2011). PIF1, PIF3, PIF4 and PIF5 have also been found to act as constitutive repressors of photomorphogenesis under dark (Leivar, Monte, Oka, et al., 2008).

1.4.2. Negative regulation of photomorphogenesis by PIFs

As members of the basic Helix-Loop-Helix transcription factor family, PIFs possess both the ability to bind directly to target gene promotors, in their basic region, and the ability to bind to photoactivated phytochromes, making them the ideal candidates for investigation of the underlying mechanisms behind light-regulated gene expression. After light activation, cytosolically localized phytochromes are translocated into the nucleus in a process that is fine-tuned by light quality and quantity (Hiltbrunner et al., 2005; Huq et al., 2003). While no consensus has been reached yet regarding the molecular mechanisms behind phyB nuclear import (Klose et al., 2015), light-labile phyA is known to enter the nucleus very rapidly through interaction with NLS-containing proteins far red elongated hypocotyl 1 (FHY1) and fhy1-like (FHL), decreasing the cytosolic level of phyA in the active Pfr conformation (Klose et al., 2015; Rausenberger et al., 2011). phyB translocation into the nucleus is not dependent on FHY1 and FHL, but may be facilitated by interaction with NLS-bearing PIFs, namely PIF1 and PIF3-5 (Pfeiffer et al., 2012). Interaction with E3 ligases then regulates the stability of three main TF families (PIFs, EIN3/EIN3-LIKE 1 (EIN3/EIL1) and LONG HYPOCOTYL 5 and its homolog (HY5/HYH)), inducing a transcriptional cascade towards photomorphogenesis (Shi et al., 2018). This reprograming leads to the inhibition of hypocotyl elongation by degradation of PIF1, PIF3, PIF4 and PIF5 (Leivar et al., 2008), apical hook unfolding, cotyledon opening and expansion due to attenuation of ethylene responses (Shi et al., 2016) and etioplast-chloroplast differentiation enabled by de-repression of expression of *LIGHT HARVESTING COMPLEX* (*LHC*) genes (Liu et al., 2017). Although photomorphogenesis has been mainly studied in the model species Arabidopsis, it is common among many plant species, including monocots, in which it is typically characterized by the inhibition of coleoptile elongation and emergence

of the first true leaf (Gommers & Monte, 2018). However, the regulatory networks underlying photomorphogenesis in different monocot plants are either yet to be or poorly characterized.

1.4.3. OsPIFs regulating rice development and rice responses to environmental cues

The interaction between Osphys and OsPIFs constitutes a regulatory hub that can perceive and integrate environmental stimuli, inducing transcriptional changes that fine-tune rice seedling growth and development. OsPIF1 (also known as OsPIF13) has been identified as a key regulatory factor of reduced plant height, as it promotes internode elongation via cell wall-related genes in response to drought stress (Todaka et al., 2012). OsPIF14 promotes mesocotyl and root growth under salt stress and dark, which are crucial for plant growth in saline soils, by directly binding to the promotor of cell elongation-related genes and regulating their expression (Mo et al., 2020). OsPIF16 has been reported to be involved in OsphyB-mediated regulation of cold tolerance (He et al., 2016) and, along with OsPIF11, it has also been shown to act as a transcriptional activator in the promotion of skotomorphogenesis and repression of photosynthesis-related genes (Li Y. et al., 2022). Finally, OsPIF15 is speculated to repress seedling growth probably by regulating the auxin pathway and suppressing cell wall organization in etiolated rice seedlings (Zhou et al., 2014).

1.5. Main objectives

Previous unpublished studies conducted at the host lab revealed that, in the dark, *OsPIF15* and *OsPIF16* are the only *OsPIF* genes that are highly expressed in WT etiolated seedlings and that the coleoptile growth of etiolated *ospif15* and *ospif16* knock-out mutants is compromised. As a longer coleoptile allows for deep seed sowing and increases plants' suitability to areas that are susceptible to drought by allowing them to take better advantage of soil moisture (Khadka et al., 2021), the compromised phenotype of these mutants ultimately hinders seedling establishment. Hence, the main aim of this work is to understand whether these are indeed the main rice PIFs involved in coleoptile elongation. If so, we will seek to unravel the regulatory mechanisms underlying the phenotype of the *ospif15* and *ospif16* mutants grown under dark and characterize the function of OsPIF15 and OsPIF16 in coleoptile growth and development of rice seedlings. To do so, we will first validate the significance of OsPIF15 and OsPIF16 in the regulation of rice coleoptile growth by growing all *ospif* mutants under different light conditions (dark, white, red and far-red light). If OsPIF15 and OsPIF16 are confirmed to be key players in the coleoptile development, we will analyze the interactions of OsPIF15 and OsPIF16 with the rice phytochromes and with each other through Bimolecular Fluorescence Complementation (BiFC) and Yeast two-Hybrid (Y2H). In addition, we will analyze OsPIF16 protein stability in response to light, in WT and *phyB-1* mutant seedlings, to understand if OsPIF16 degradation occurs in a phyB-dependent manner. This has already been investigated for OsPIF15 (Xie et al., 2019). Furthermore, transgenic rice plants overexpressing either OsPIF15 or OsPIF16 (in fusion with a protein tag) will be produced as a tool for future analysis of OsPIF15 and OsPIF16 degradation under different light

conditions, identification / validation of protein-protein interactions (between these TFs and with phytochromes) as well as identification of their DNA targets.

2. Materials and Methods

2.1. Production of rice transgenic lines

The multistep rice transformation protocol used for production of rice transgenic lines during this MSc project is summarized in **Figure 2.1.** and will be described in detail in this section.

2.1.1. Plant material and growth conditions

The japonica rice cultivar *Oryza sativa* L. cv. Nipponbare was used for transformation. The compositions of the media used for rice transformation are listed in **Table S1** and **Table S2** . The wild type plants used for transformation and the regenerated transgenic rice plants were grown in soil (composed of peat moss, soil and vermiculite in a 2:2:1 ratio), at 28°C, 70% RH, under a 12h/12h light/dark photoperiod.

2.1.2. Agrobacterium transformation

The Gateway destination vectors required to produce the transgenic rice plants overexpressing either OsPIF15 (OsPIF15-OX-Myc) or OsPIF16 (OsPIF16-OX-Myc) were generated in the host lab prior to the start of this MSc project. Once these constructs, carrying either *OsPIF15*-CDS or *OsPIF16*-CDS in fusion with a Myc tag and under the control of the maize ubiquitin (Zm*Ubi-1*) gene promotor, were created, they were individually transformed into the *Agrobacterium tumefaciens* strain EHA105 following the heat shock method, and grown for 3 days in MYB medium supplemented with rifampicin (25 µg/mL) and spectinomycin (100 µg/mL). The transformation of the *A. tumefaciens* colonies grown on the selection medium was analyzed by colony PCR (polymerase chain reaction), using GoTaq G2 Flexi DNA polymerase (Promega, USA) and a pair of primers that amplify a fragment of the *hpt*II (hygromycin resistance gene) marker gene. HptII-positive colonies were streaked in new MYB plates with the same antibiotics. After another 3-day incubation at 28 °C in the dark, the transformed agrobacterium was used for rice transformation.

2.1.3. Rice transformation

An agrobacterium colony transformed with OsPIF15-OX-Myc and one transformed with OsPIF16-OX-Myc were picked from their respective plates and separately suspended in a co-cultivation medium liquid (CCML) solution with 1:1000 acetosyringone (100 µM) until an OD_{600} of 0.65 - 0.70 was reached. The resulting agrobacterium cell suspensions were used for transformation of Nipponbare rice *calli* dedifferentiated from mature seed, via a modified version of the protocol described in Hiei et al., 1994. Briefly, de-husked rice seeds were surface-sterilized with 1g/L Benlate (Sigma-Aldrich, USA) for 30 min in a 50°C water bath, rinsed with ddH_2O two times and further sterilized with 10 mL of 70% ethanol for 2 min and 1 drop of Tween® 20 (Sigma-Aldrich, USA)/10 mL of 50% bleach for 10 min with stirring.

From this point, until the transfer of regenerated seedlings to soil, all tissue manipulation was performed inside a laminar air flow (LAF) chamber. First, de-husked seeds were washed 6 to 8 times with autoclaved ddH_2O, plated in *callus* inducing medium (CIM), and incubated in the dark at 28°C. After 14 days, the *scutella* tissue was separated from the seeds and placed in new CIM plates for another 14 days in the same conditions. From this tissue, selection of embryogenic *calli* was performed. After 5 days in new CIM, the *calli* were immersed in the above-mentioned agrobacterium suspensions for 15 min with agitation, and subsequently incubated without rinsing in co-cultivation medium solid (CCMS) plates with sterilized filter paper to soak the excess agrobacterium, for 3 days at room temperature (RT) in the dark. From this step on, the *calli* that remained alive and showed no agrobacterium overgrowth were subjected to three steps of selection in selection medium (SM) with 50 mg/L hygromycin, two steps of embryogenic improvement in embryogenic improvement medium (EIM) with 100mg/L hygromycin and 4 to 8 regeneration steps in regeneration medium (RM). The plantlets that regenerated from the hygromycin-resistant *calli* were transferred to plantlet development medium (PDM) with 25 mg/L hygromycin. Once their shoots were longer than 5 cm, regenerated plantlets were transferred to 2 L pots of soil (composed of peat moss, soil and vermiculite in a 2:2:1 ratio). To check whether the regenerated rice plants were indeed transformed, leaf samples were collected, and genomic DNA was extracted using 20 µL of the QuickExtract™ DNA Extraction Solution (Lucigen Cooperation, Middleton, WI, USA), following the manufacturer's procedure. PCR was performed using GoTaq G2 Flexi DNA polymerase (Promega, USA) and the hptII primer pair for amplification.

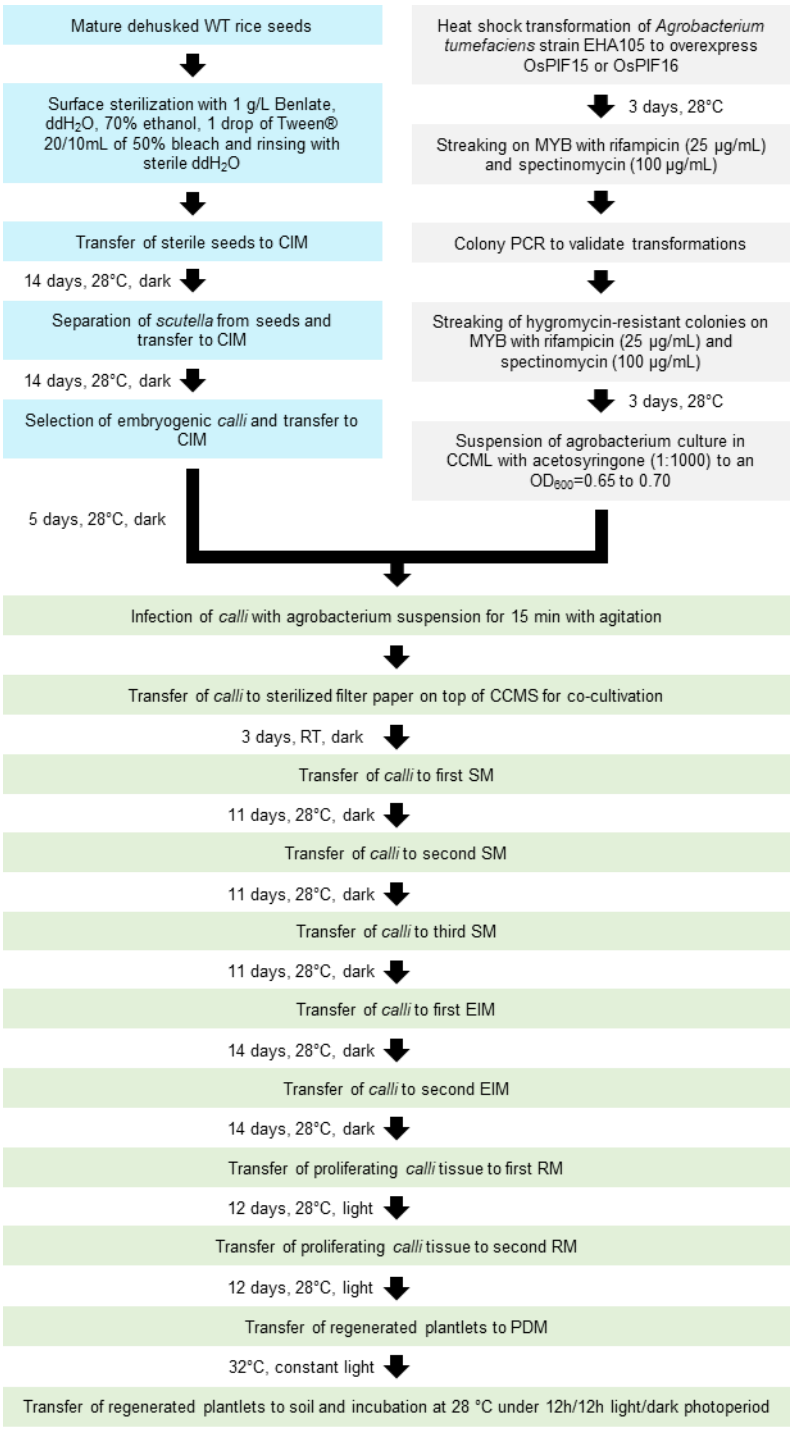

Figure 2.1 Workflow of the protocol for rice transformation. Adapted from Sahoo et al., 2011.

2.2. Yeast Two-Hybrid

All bait and pray vectors used for Yeast two-Hybrid (Y2H) were generated in the host lab prior to the start of this MSc project. The combinations between the pGAD or pGBK empty vectors and each of the constructs tested were employed as negative controls. *Saccharomyces cerevisiae* Y2HGold strain (Clontech, USA) was transformed with each bait and prey vector combination, following the LiAc/PEG-

mediated transformation protocol detailed in the Yeastmaker™ Yeast Transformation System 2 User Manual (Clontech). First, yeast cells were incubated in YPDA medium O/N at 30°C, 180 rpm, until an OD_{600} of 0.4 to 0.8 was reached. Competent yeast cells were prepared by centrifuging the O/N cell cultures at RT, 2000 rpm, for 5 min, discarding the supernatant, and resuspending the pellet in autoclaved ddH_2O; centrifuging again in the same conditions, discarding the supernatant and resuspending the pellet in 1.1x TE/LiAc (10 mM Tris-HCl, pH 7.5; 1 mM EDTA, pH 7.5/100 mM lithium acetate, pH 7.5); and finally, centrifuging at high speed for 15 s, discarding the supernatant and resuspending the pellet in 1.1x TE/LiAc. The competent cells were then transformed with each vector combination (pGAD and pGBK). In brief, the cells were incubated with the plasmid combinations, PEG/LiAc solution and denatured Yeastmaker Carrier DNA (Takara, Japan) at 30°C for 30 min, heat-shocked at 42°C for 15 min, pelleted at 14800 x *g* for 15 s, resuspended in 1X TE and plated in synthetic defined (SD) medium without leucine (L) and tryptophan (T) (SD-L-T). After a 3-day incubation at 30°C, 4 colonies of each transformation were re-streaked in new SD-L-T plates. Following another 3-day incubation, 2 colonies of each transformation were tested by yeast cell spotting as following: each colony was grown O/N in liquid SD supplemented with leucine and tryptophan, diluted to an OD_{600} of 0.4, centrifuged at 14800 x *g* for 30 s and washed with SD twice. The resulting cell suspensions were used to prepare serial dilutions of 1:10 and 1:100, and 5 µL of each were plated in control (SD-L-T) and test plates (SD-L-T-H; SD-L-T-H + 1mM 3-amino-1, 2, 4-triazole (3-AT); SD-L-T-histidine(H)-adenine(A)). The plates were then incubated at 30°C for 3 days.

This technique relies on the expression of a reporter gene, which is activated by the interaction of the GAL4 DNA-binding domain (BD) present in the bait plasmid and the GAL4 activation domain (AD) present in the prey plasmid, when this is promoted by the interactions of two proteins independently fused to a BD and an AD. The bait plasmid contains the *TRP1* gene, and the prey plasmid contains the *LEU2* gene, which are part of the tryptophan and leucine biosynthetic pathways, respectively. Hence, only yeast cells transformed with both plasmids can grow on medium lacking both amino acids. The yeast strain used in this assay (Y2HGold) contains a *HIS3* reporter gene that is involved in the histidine biosynthetic pathway and the binding of the GAL4 TF domains enables GAL4-responsive *HIS3* expression, allowing yeast cells to biosynthesize histidine and grow on minimal medium lacking this essential amino acid. If the reporter gene is not activated, the yeast strain cannot grow unless provided with histidine. Thus, yeast cells were plated on SD-L-T+H+A (control plate) and on SD-L-T-H+A, SD-L-T-H+A + 1 mM 3-AT and SD-L-T-H-A (test plates of increasing stringency, respectively). 3-AT is a competitive inhibitor of the *HIS3* reporter gene product and it is used to titrate the minimum level of *HIS3* expression required for growth on histidine-deficient medium, thus controlling growth resulting from self-activation of the *HIS3* reporter gene instead of bait activation (Tian et al., 2012). In addition, Y2HGold is also auxotrophic for adenine, containing the ADE2 reporter gene (under the control of the GAL4 UPS), which is essential for adenine biosynthesis and provides stronger nutritional selection than *HIS3* (*Matchmaker ® Gold Yeast Two-Hybrid System User Manual*, n.d.). Thus, only the results for yeast growth on control medium and medium lacking all four amino acids will be shown.

2.3. Bimolecular Fluorescence Complementation

2.3.1. Preparation of agrobacterium strains for agroinfiltration

Prior to the start of this MSc project, the coding regions of *OsPIF15* and *OsPIF16* as well as the non-photoactive C-terminal domains of *OsphyA*, *OsphyB* and *OsphyC* were individually cloned in both pYFN^{C}43 and YFP^{N}43 (Belda-Palazón et al., 2012), in order to test the interactions between Osphys and OsPIFs by bimolecular fluorescence complementation (BiFC). Each construct was introduced into the *A. tumefaciens* strain EHA105, using the heat shock method and grown in MYB plates with rifampicin (25 µg/mL) and kanamycin (50 µg/mL). The transformations were confirmed by colony PCR (as described in **section 2.1.3 of Materials and Methods**) and the HptII-positive colonies harboring each construct were inoculated in 5 mL of Luria-Bertani (LB) medium with rifampicin and kanamycin and grown O/N at 28°C, 180 rpm. Agrobacterium harboring the P19 vector was grown concomitantly in the same conditions. After a 5 min centrifugation at 2000 x *g*, the resulting pellets were resuspended in 10 mL of infiltration buffer (10 mM $MgCl_2$, 10 mM MES pH 5.6) and, following a second centrifugation in the same conditions, the pellets were resuspended in 10 mL of infiltration buffer supplemented with 100 µM acetosyringone (Sigma-Aldrich, USA). The OD_{600} of each cell suspension was measured and the respective volumes required to achieve an OD_{600}=0.2 (or OD_{600}=0.1 for the culture harboring the P19 vector) were calculated. The desired combinations were then prepared by adding the volumes of the two cell suspensions and the P19 vector culture and making up the desired final volume with infiltration buffer. Before agroinfiltration, the resulting agrobacterium cell suspensions were grown at RT in the dark, for 2h, to induce virulence.

2.3.2. Agroinfiltration of *Nicotiana benthamiana* leaves

Wild Type (WT) *Nicotiana benthamiana* seeds were subjected to a -4°C stratification for 3 days and sown in pots containing a mixture of Siro Royal substrate (Siro, Portugal) and vermiculite in a 5:1 ratio. Once the first leaf emerged, the seedlings were transferred to individual pots and grown at 22°C under a 12h/12h light/dark cycle (light intensity of 80-100 µmol m^{-2} s^{-1}). Each agrobacterium mixture was infiltrated into the abaxial epidermis of 5-week-old *N. benthamiana* leaves using needless syringes. Each combination was used to infiltrate an entire leaf. After 2 days growing under a 12h/12h light/dark photoperiod, the plants were transferred to continuous dark for 18-20h to induce OsPIF accumulation, and then leaf disks were harvested. The empty vectors pYFN^{C}43 and pYFN^{N}43 were combined with each gene construct tested (in a complimentary manner) to serve as negative controls.

2.3.3. Fluorescence microscopy

YFP fluorescence was examined under a Leica DM6 B Upright fluorescence microscope (40x) with L5 filter cube (Leica, Germany). ImageJ (National Institutes of Health, USA) was used to merge brightfield and fluorescence images.

2.4. Coleoptile growth assays

2.4.1. Plant material and growth conditions

All CRISPR/Cas9 knock-out mutants used for these growth assays (*ospif11*, *ospif12*, *ospif13*, *ospif14*, *ospif15*, *ospif16*, *ospif8,* and *ospif15&16*) had been previously developed in the host lab (**Table S3**). Seeds from three independent lines of each mutant were grown together with WT rice (*O. sativa* L. cv. Nipponbare) in a walk-in growth chamber under a 12h/12h light/dark cycle (light intensity of 500 µmol m^{-2} s^{-1}), at 28°C / 24ºC (light/dark), in soil, and the new seeds were harvested. Genomic DNA samples from each plant line were collected for Sanger sequencing analysis and homozygous lines were used for phenotypical analysis. For each assay, 40 seeds from the abovementioned amplification session of each plant line were incubated in polypropylene tissue culture boxes with a paper towel on the bottom and 40 mL of double distilled water (ddH_2O). Continuous darkness (Dc), white (Wc, 100 µmol m^{-2} s^{-1}), red (Rc, 15 µmol m^{-2} s^{-}1) and far-red (FRc, 15 µmol m^{-2} s^{-1}) light were tested. The seedlings were grown for 9 days (under dark) or 7 days (under all light conditions), inside a FitoClima 1200 Bio plant growth "reach in" chamber (Aralab, Portugal), at 28°C. Light shelves with 4 cool-white LED tubes were used for growth under Wc light, while Rc and FRc light were supplied by R or FR light-emitting diodes (LEDs), respectively. Coleoptile growth assays under Dc and Wc light, were performed 4 and 3 times, respectively. Rc and FRc light assays were performed twice.

2.4.2. Coleoptile measurements and statistics

Images of the seedlings grown under Wc, Rc or FRc light were captured 7 days after incubation, while those of seedlings grown in darkness were captured 9 days after incubation, using the camera of a Huawei P30 Pro. Each image comprising all the seedlings of a singular plant line, was individually captured and a ruler included in each photograph was used to set the scale during image analysis. Coleoptile measurements were taken using ImageJ (National Institutes of Health, USA) and only opened coleoptiles were measured. GraphPad Prism 8.0.2 (GraphPad Software Inc., California, USA) for Windows was used to perform statistical data analysis and data visualization. Outlier detection was carried out in GraphPad Prism using the ROUT method (robust regression followed by outlier identification) with the ROUT coefficient (Q) set to 10%. Coleoptile length data were analyzed by ordinary one-way analysis of variance (ANOVA). Dunnett's multiple comparisons test was used to calculate the mean difference between each genotype and the WT or between different light conditions. Mean differences with a *P* value<0.01 were defined as statistically significant and are denoted by an asterisk (*).

2.5. OsPIF16 protein degradation assay

2.5.1. Plant materials and growth conditions

To check if OsPIF16 is degraded after light exposure in WT and *ospif* mutants, fifty seeds from three independent lines of each of the CRISPR/Cas9 knock-out single mutants previously developed in the host lab (*ospif11*, *ospif12*, *ospif13*, *ospif14*, *ospif15*, *ospif16* and *ospif8*) and WT rice (*O. sativa* L. cv. Nipponbare) were surface-sterilized (as described in **section 2.1.3 of Materials and Methods**) and incubated in sterile polypropylene tissue culture boxes with a paper towel on the bottom and 40 mL of ddH_2O, in the dark at 28°C. One of two boxes containing WT seedlings was transferred to white light (100 µmol m^{-2} s^{-1}) 24h prior to plant tissue sample collection to be used as negative control. The aerial portion of 8-day-old etiolated rice seedlings was cut above the mesocotyl using a scalpel (under green light), flash frozen in liquid nitrogen and stored at -80°C. The amount of plant tissue collected was enough to fill two 1.5 mL Eppendorf tubes. The *ospif12* sample was not collected due to seedling contamination. To check if OsPIF16 degradation by light is mediated by OsphyB, the same sterilization protocol was used for de-husked WT and *osphyB-1* mutant seeds, which were then incubated in the same abovementioned conditions. After 8 days under dark, the seedlings were transferred to Wc light (100 µmol m^{-2} s^{-1}) and their aerial portions were collected at six different timepoints of light exposure (0h, 30 min, 1h, 3h, 6h and 9h).

2.5.2. Protein extraction and detection of OsPIF16 by Western blotting

The collected plant tissue samples of WT and knock-out mutant seedlings were macerated inside Eppendorf tubes using small pestles, until a fine powder was obtained. Total protein extraction was performed by adding 150 µL of 2X Laemmli buffer (1 M Tris-HCl, pH 6.8, 4% SDS, 20% (w/v) glycerol, 0.01% bromophenol blue; Bio-Rad, USA) supplemented with 50 mM DTT to 50 mg of macerated tissue. The resulting suspensions were incubated at 70°C for 10 min, centrifuged at -4°C, 20000 x *g*, for 10 min, and the resulting supernatants collected. The last two steps were repeated. Proteins were separated by running protein samples (5 µL) in sodium dodecyl sulphate-polyacrylamide gel electrophoresis (SDS-PAGE) (10%) at 60 V. These proteins were then transferred to a polyvinylidene fluoride (PVDF) membrane (Bio-Rad, California, USA) applying a voltage of 30 V for O/N at 4°C. As a loading control, the membrane with the blotted proteins was stained with Ponceau S stock solution and photographed. The membrane was then blocked with 5% skim milk in Tris Buffer Saline with 2 % Tween® 20 (TBS-T) for 1h at RT and incubated for 1h at RT with the primary antibody α-OsPIF16 (1:2000 dilution in blocking solution; Abbexa, USA). After three washes with TBS-T, the membrane was incubated with the secondary antibody α-rabbit conjugated with HRP (1:20000 dilution in blocking solution; Novex, USA) for 1h at RT, and washed again three times with TBS-T. The detection was performed using the enhanced chemiluminescence (ECL) Western blotting detecting reagent (Amersham™, UK) and the images were acquired with iBright™ FL1500 Imaging System (Thermo Fisher Scientific). The protocol followed for the tissue samples of WT and *osphyB-1* mutants was similar to what is described above, with some modifications: the gel was run at 200 V; protein transfer was

performed using nitrocellulose membranes (Amersham™, UK) and applying a voltage of 100 V for 1h at RT; and the membrane was incubated O/N at 4°C with the primary antibody. To detect β-tubulin, which served as loading control, the blot was stripped with TBS-T O/N at 4 ºC, incubated with the α-β-tubulin antibody (1:1000; Santa Cruz Biotechnology, USA) in 1 % skim milk in TBS O/N at 4 ºC, and the α-mouse antibody conjugated with HRP (1:20000; Amersham™, UK) for 1 h at RT. The detection was performed as described above for α-OsPIF16.

3. Results and Discussion

3.1. Are OsPIF15 and OsPIF16 key regulators of rice coleoptile development?

While the roles of Arabidopsis PIFs in phytochrome-mediated photoresponses have been widely reported (Huq et al., 2004; Huq & Quail, 2002; Khanna et al., 2004; Leivar, Monte, Al-Sady, et al., 2008; Luo et al., 2014; Ni et al., 1999; E. Oh et al., 2004; J. Oh et al., 2020), the phytochrome-mediated signal transduction network of rice remains fairly unknown. One of the main goals of the host lab (PGR at ITQB NOVA) is to unveil the role of rice Phytochrome-Interacting Factors (PIFs) in the regulation of skotomorphogenesis by studying coleoptile growth. Preliminary studies conducted in this lab suggest that, under dark, the coleoptile growth of *ospif15* and *ospif16* knock-out mutants is significantly compromised compared to WT seedlings, and that *OsPIF15* and *OsPIF16* are the most highly expressed *OsPIF* genes in etiolated rice seedlings. Furthermore, these two transcription factors have been found to share a close genetic relationship (Ji et al., 2019; Nakamura et al., 2007b). Thus, in the following assays, three independent lines of each *ospif* CRISPR/Cas-9 knock-out rice single (*ospif11*, *ospif12*, *ospif13*, *ospif14*, *ospif15*, *ospif16*, *ospif8*) and double (*ospif15 ospif16*) mutants were grown under different light conditions (continuous dark (Dc), white (Wc), red (Rc) and far-red (FRc) light), along with the WT, to assess the role of the different OsPIFs in the regulation of plant growth and development.

3.1.1. Dark-grown *ospif15*, *ospif16* and *ospif15 ospif16* mutants show impaired coleoptile growth

In order to identify the OsPIFs that play a major role in the regulation of rice skotomorphogenesis, all *ospif* mutant lines were grown in three independent experimental replicates under constant dark, and an additional assay was conducted for the *ospif16* mutant lines. After 9 days under constant dark, all three lines for both *ospif15* single and *ospif15 ospif16* double mutant developed significantly shorter coleoptiles than the WT in all replicates, whereas the three *ospif16* lines grew significantly shorter coleoptiles in all but the third replicate (**Figure 3.1 a-c**). Given the inconsistency regarding the *ospif16* mutant within the three assays, and considering the above-mentioned previous studies, a fourth assay using only the WT and *ospif16* lines was performed. This assay confirmed that coleoptile development is indeed significantly compromised in the *ospif16* mutant (**Figure 3.1 d**).

It has been reported that Dc-grown transgenic rice seedlings overexpressing *OsPIF15* (*OsPIF15*-OX) show impaired above-ground development, namely shorter coleoptiles and leaves, than the WT, but coleoptile growth is similar when both are grown under Rc of FRc. These results show that OsPIF15 plays a role in coleoptile growth regulation and might be degraded by light (Zhou et al., 2014). Because *OsPIF15* expression is increased by at least 20-fold in the *OsPIF15*-OX lines compared with to WT, the authors speculated that this high accumulation of OsPIF15 might play a pleotropic effect in rice development, thus used R light pulses to decrease the amount of OsPIF15. They observed that, when WT and *OsPIF15*-OX are grown under Dc and subjected to R light pulses every 12h, the seedlings develop, respectively, shorter, and longer coleoptiles. The authors hypothesize that, when *OsPIF15*-OX seedlings are subjected to a R light pulse, the OsPIF15 protein decreases to a threshold level similar to that of WT. While the re-accumulation of OsPIF15 in *OsPIF15*-OX seedlings in the dark period following the light pulse is sufficient to inhibit seedling growth without having the pleiotropic effect, in WT seedlings, this accumulation is slower and coleoptile length is similar to constant light conditions. This shows that OsPIF15 represses skotomorphogenic development of rice seedlings when highly accumulated, but, once its protein levels are slightly higher than the basal level, it promotes skotomorphogenesis (Zhou et al., 2014), which is consistent with our observations regarding the *ospif15* mutant. Additionally, a study in which *OsPIF16* was fused with the SRDX repression domain to act as a transcriptional repressor, and the *OsPIF16-SRDX* fusion construct was expressed in WT rice plants grown under dark, resulted in transgenic plants presenting constitutively photomorphogenic phenotype, suggesting that OsPIF16 also acts as a transcriptional activator to maintain skotomorphogenesis (Y. Li et al., 2022), supporting our results in which a lack of OsPIF16 protein translated into reduced coleoptile growth. Our study shows that while the reduction in coleoptile length compared to the WT was bigger in the *ospif15* lines than in the *ospif16* mutants, the greatest difference was observed in the *ospif15 ospif16* double mutants (**Figure 3.1 e**). Thus, we hypothesize that OsPIF15 and OsPIF16 act in a non-redundant manner, with OsPIF15 likely regulating most of the genes involved in coleoptile development and elongation, while OsPIF16 plays a much smaller but still relevant role, as supported by the synergistic effect observed in the double mutant lines when both genes are knocked out.

In contrast to our lab's previous results, here, the difference in coleoptile length between single mutant lines and the WT was not exclusive to the *ospif15* and *ospif16* mutants. In two of the growth assay replicates, at least one of the *ospif11*, *ospif12* and *ospif13* lines grew significantly shorter coleoptiles than the WT, while for *ospif14*, at least one of the lines grew significantly shorter coleoptiles than the WT in all assay replicates (**Figure 3.1 a-c**). Although the ability of OsPIF12, OsPIF13 and OsPIF14 to affect the etiolated coleoptile growth has not been shown before, the same study mentioned above for OsPIF16, showed that *OsPIF11* fused with the transcriptional repressor SRDX and overexpressed in WT rice plants results in shorter coleoptile growth under dark (Y. Li et al., 2022). These results, together with our observations, indicate that OsPIF11 may also play an important role in coleoptile elongation. The *ospif8* mutant showed no significant differences in coleoptile elongation compared to the WT, except for *ospif8.1* in the third assay. Since this assay, however, seems to notably diverge from the remaining replicates, we suspect that an error may have occurred unbeknownst to us. Altogether, our results suggest that, although OsPIF15 and OsPIF16 seem to be the key players in

assuring the correct growth and development of rice coleoptiles, other OsPIFs may also influence this process. However, since the mutants lacking these OsPIFs showed inconsistent coleoptile growth, further replicates need to be produced to confirm their phenotype. Moreover, the development of double and triple mutants such as *ospif15 ospif11*, *ospif16 ospif11* and *ospif15 ospif16 ospif11* could also be useful to further assess whether other OsPIFs, such as OsPIF11, play a role in rice coleoptile development.

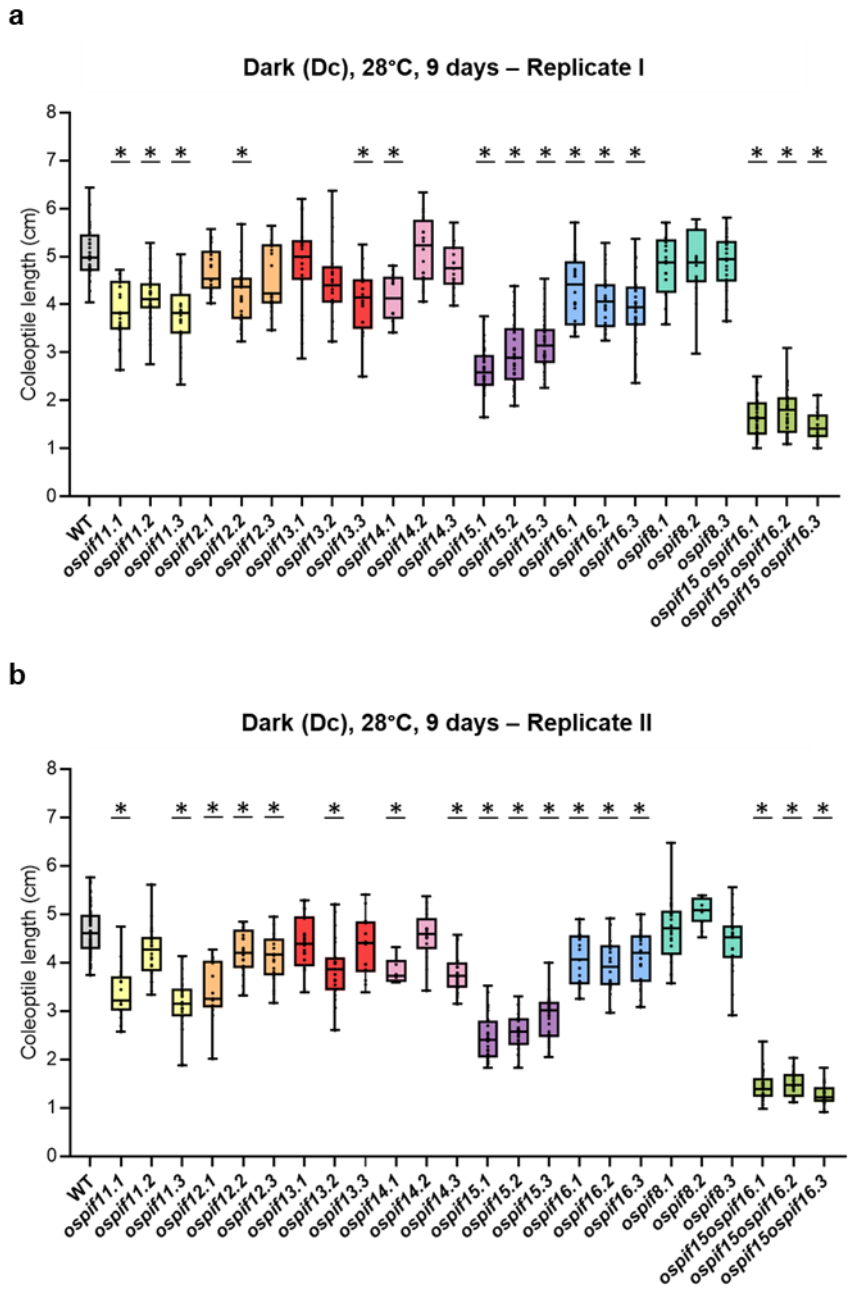

Figure 3.1 Analysis of rice coleoptile length in WT and *ospif* mutants grown under dark. Coleoptile length (in cm) was assessed in 9-day-old rice seedlings. WT (grey) and *ospif* mutants (each color represents three independent lines of the same mutant) were grown at 28°C, under constant dark (Dc). Three experimental replicates **(a-c)** were performed, and an additional growth assay **(d)** was performed to confirm the phenotype of *ospif16* mutants under dark. Asterisk (*) denotes a significant difference ($p < 0.01$) between WT and *ospif* seedlings according to a one-way ANOVA followed by a Dunnett's multiple comparisons test. For **a-d**, respectively, $13 \leq n \leq 39$, $7 \leq n \leq 63$, $13 \leq n \leq 86$, and $12 \leq n \leq 25$. **(e)** Representative photographs of 9-day-old etiolated rice seedlings composed of the roots and aerial part, which includes the mesocotyl, the coleoptile (shown in between white arrowheads) and leaves. Scale bar, 1 cm.

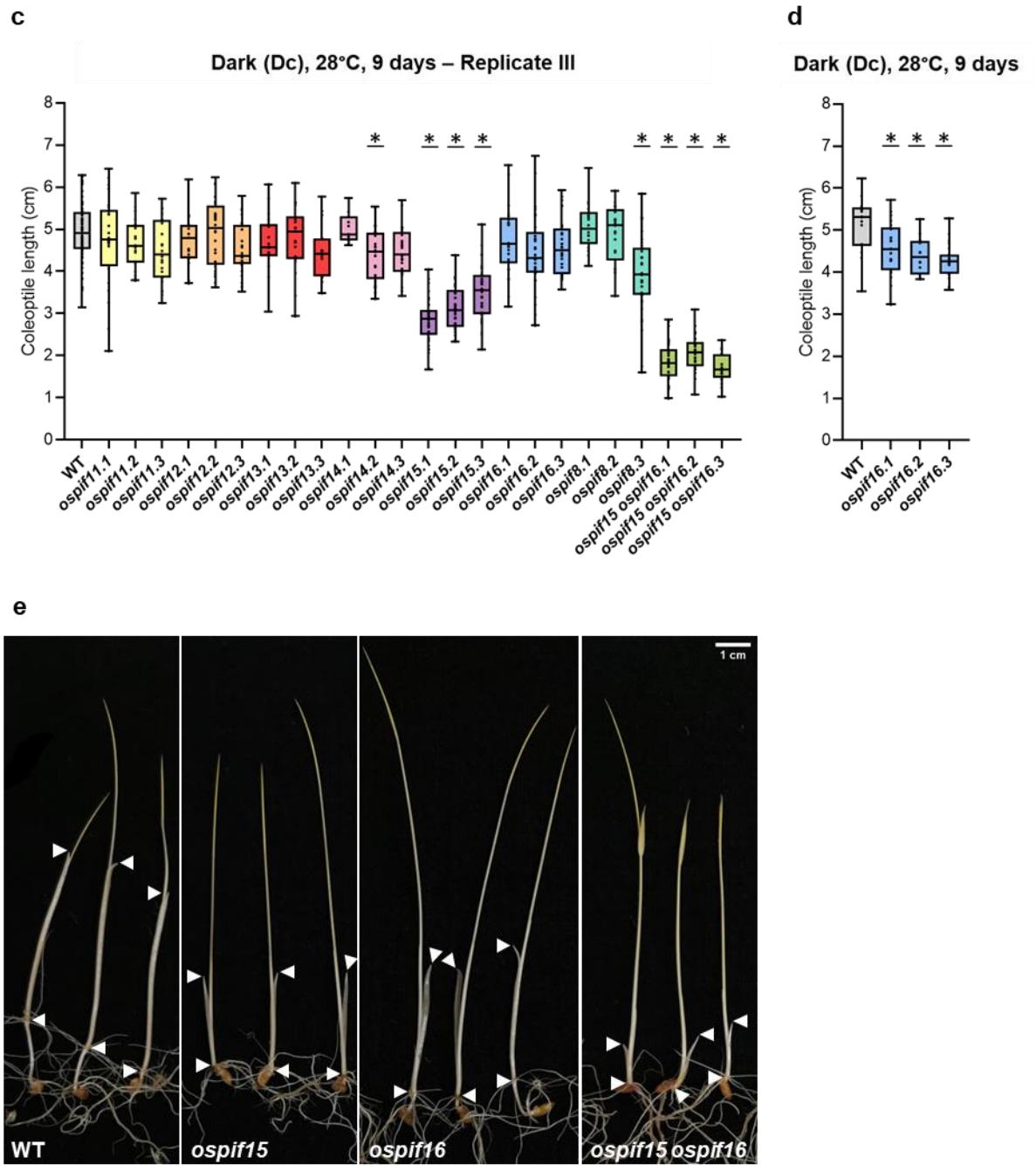

Figure 3.1 (Continued) Analysis of rice coleoptile length in WT and *ospif* mutants grown under dark. Coleoptile length (in cm) was assessed in 9-day-old rice seedlings. WT (grey) and *ospif* mutants (each color represents three independent lines of the same mutant) were grown at 28°C, under constant dark (Dc). Three experimental replicates **(a-c)** were performed, and an additional growth assay **(d)** was performed to confirm the phenotype of *ospif16* mutants under dark. Asterisk (*) denotes a significant difference ($p < 0.01$) between WT and *ospif* seedlings according to a one-way ANOVA followed by a Dunnett's multiple comparisons test. For **a-d**, respectively, $13 \leq n \leq 39$, $7 \leq n \leq 63$, $13 \leq n \leq 86$, and $12 \leq n \leq 25$. **(e)** Representative photographs of 9-day-old etiolated rice seedlings composed of the roots and aerial part, which includes the mesocotyl, the coleoptile (shown in between white arrowheads) and leaves. Scale bar, 1 cm.

3.2. Coleoptile growth under Wc, Rc and FRc light is similar to the WT in single and double mutants

In dark-grown seedlings, phytochromes are present in the inactive Pr form and the absence of phy activation enables PIF accumulation and skotomorphogenesis. In rice, all seven PIFs possess the phytochrome B binding domain (APB) but the interaction with OsphyB has only been confirmed for OsPIF14, OsPIF15 and OsPIF16 (Cordeiro et al., 2016; He et al., 2016; Xie et al., 2019). OsPIF15 and OsPIF16 also possess the phytochrome A binding domain (APA), but their interaction with OsphyA has not been reported. To understand the importance of OsPIFs for photomorphogenesis, WT, *ospif* single mutants and *ospif15 ospif16* double mutant seedlings were grown under continuous white (Wc; 100 µmol m^{-2} s^{-1}), red (Rc; 15 µmol m^{-2} s^{-1}) and far-red (FRc; 15 µmol m^{-2} s^{-1}) light for 7 days. Each assay was performed twice. Most mutants showed no significant differences in coleoptile elongation compared to the WT regardless of the light conditions. Under Wc light, the *ospif15 ospif16.1* line developed significantly longer coleoptiles than the WT in the first replicate (**Figure 3.2 a**), while in the second replicate, the same was true for *ospif13.2*, *ospif15.1* and *ospif8.1*, as well as the three *ospif15 ospif16* lines (**Figure 3.2 b**). Given the latter result, a third growth assay was carried out using the WT and three *ospif15 ospif16* double mutant lines, and none of the mutants showed significant differences compared to the WT (**Figure 3.2 c**). Apart from *ospif12.*2, which developed longer coleoptiles than the WT in one replicate, no mutant seedlings grown under Rc light exhibited significant differences in coleoptile length relative to the WT (**Figure 3.3**). Under FRc light, *ospif15.3* and *ospif15 ospif16.1* seedlings developed, respectively, longer and shorter coleoptiles than the WT in one of two replicates (**Figure 3.4**). In general, no statistical differences were found between the mutants and the WT in any of the three light conditions, with all mutant lines displaying short coleoptiles, characteristic of photomorphogenic development.

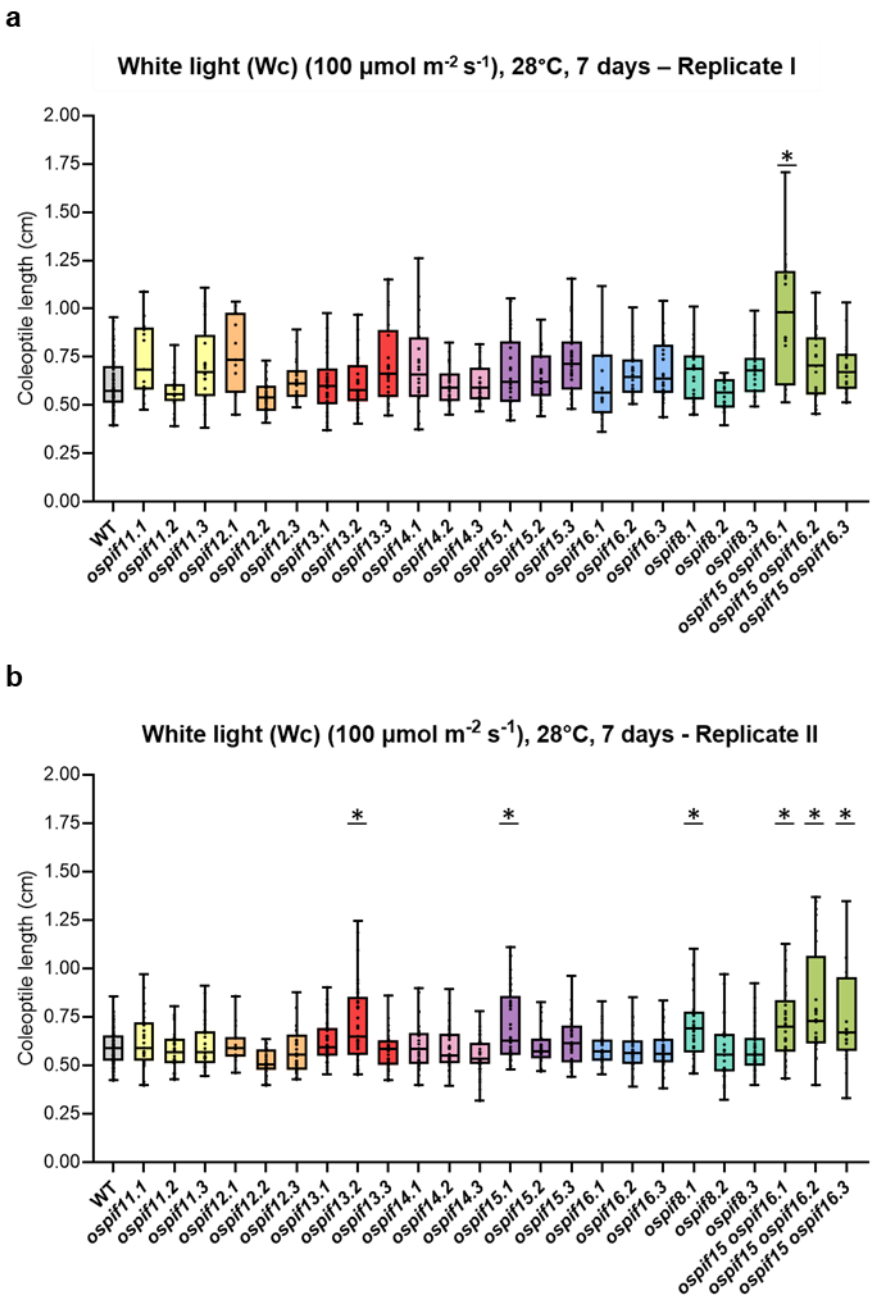

Figure 3.2 Analysis of rice coleoptile length in WT and *ospif* mutants grown under white light. Coleoptile length (in cm) was assessed in 7-day-old rice seedlings. WT (grey) and *ospif* mutants (each color represents three independent lines of the same mutant) were grown at 28°C, under constant white light (Wc; 100 µmol m^{-2} s^{-1}). Two experimental replicates **(a-b)** were performed, and an additional growth assay **(c)** was performed to confirm the phenotype of *ospif15 ospif16* mutants under white light. Asterisk (*) denotes a significant difference ($p < 0.01$) between WT and *ospif* seedlings according to a one-way ANOVA followed by a Dunnett's multiple comparisons test. For **a-c**, respectively, $13 \leq n \leq 76$, $18 \leq n \leq 111$ and $22 \leq n \leq 40$.

c

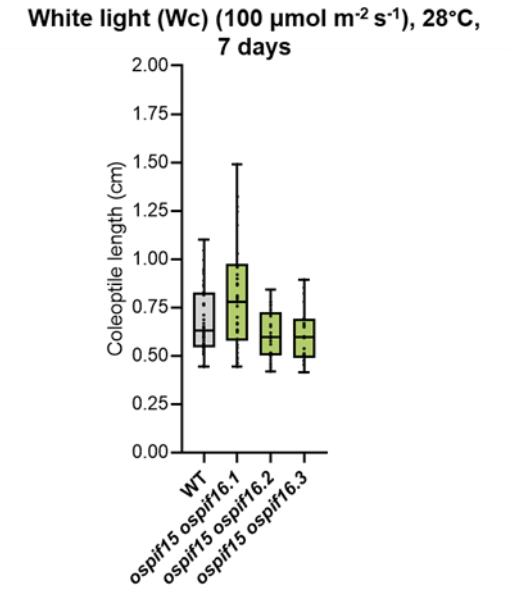

Figure 3.2 (Continued) Analysis of rice coleoptile length in WT and *ospif* mutants grown under white light. Coleoptile length (in cm) was assessed in 7-day-old rice seedlings. WT (grey) and *ospif* mutants (each color represents three independent lines of the same mutant) were grown at 28°C, under constant white light (Wc; 100 µmol m^{-2} s^{-1}). Two experimental replicates **(a-b)** were performed, and an additional growth assay **(c)** was performed to confirm the phenotype of *ospif15 ospif16* mutants under white light. Asterisk (*) denotes a significant difference ($p < 0.01$) between WT and *ospif* seedlings according to a one-way ANOVA followed by a Dunnett's multiple comparisons test. For **a-c**, respectively, $13 \leq n \leq 76$, $18 \leq n \leq 111$ and $22 \leq n \leq 40$.

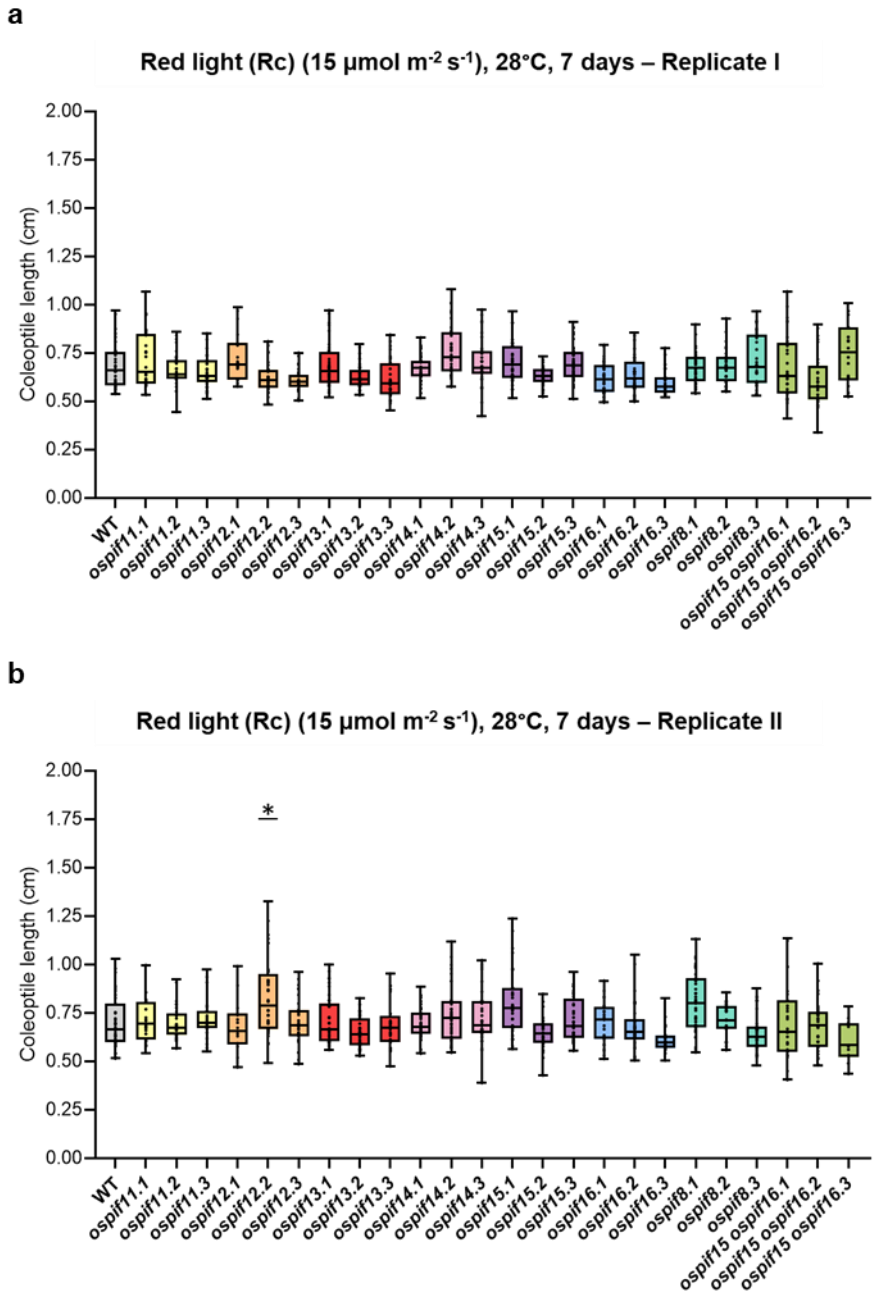

Figure 3.3 Analysis of rice coleoptile length in WT and *ospif* mutants grown under red light. Coleoptile length (in cm) was assessed in 7-day-old rice seedlings. WT (grey) and *ospif* mutants (each color represents three independent lines of the same mutant) were grown at 28°C, under constant red light (Rc; 15 µmol m^{-2} s^{-1}). Two experimental replicates **(a-b)** were performed. Asterisk (*) denotes a significant difference ($p < 0.01$) between WT and *ospif* seedlings according to a one-way ANOVA followed by a Dunnett's multiple comparisons test. For **a-b**, respectively, $18 \leq n \leq 40$ and $14 \leq n \leq 39$.

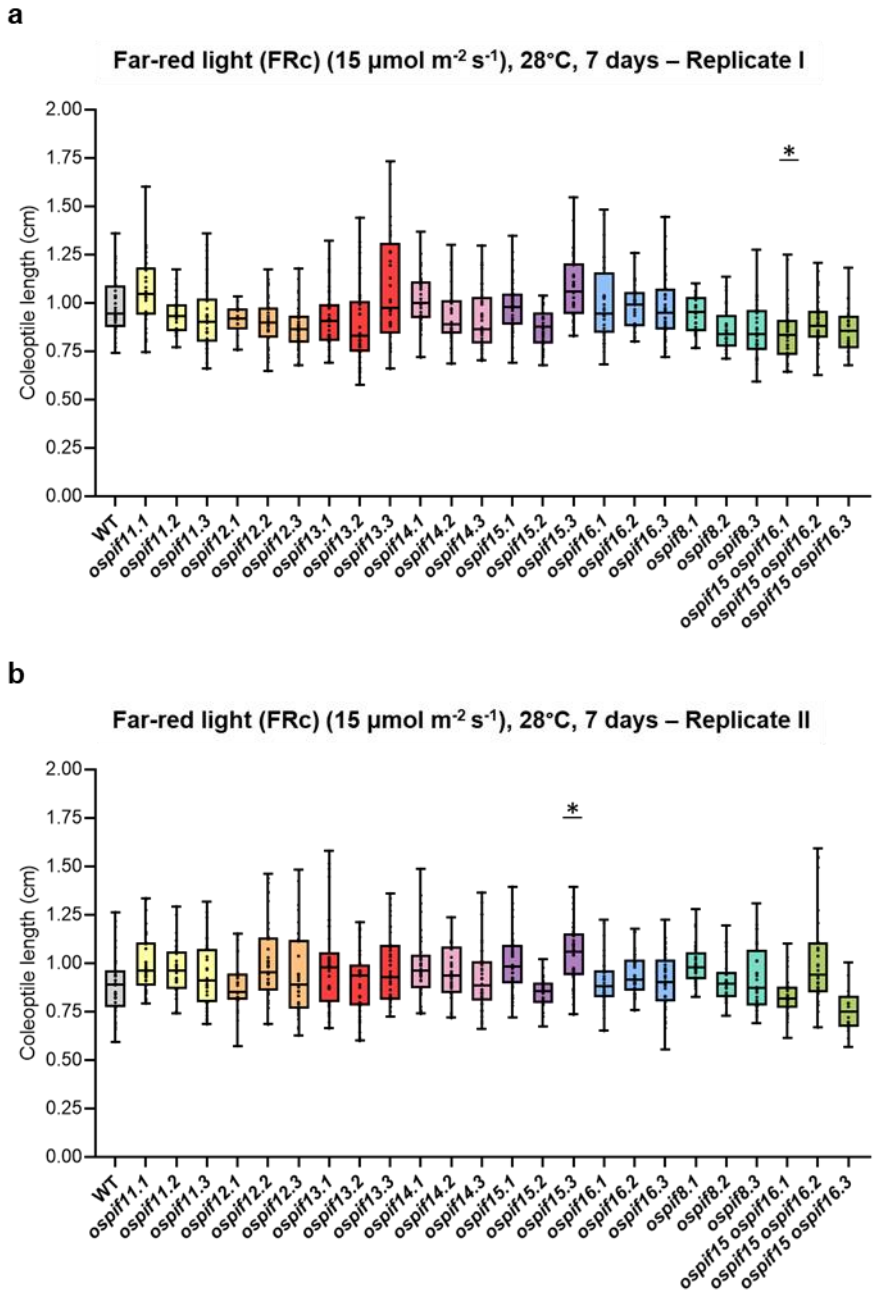

Figure 3.4 Analysis of rice coleoptile length in WT and *ospif* mutants grown under far-red light. Coleoptile length (in cm) was assessed in 7-day-old rice seedlings. WT (grey) and *ospif* mutants (each color represents three independent lines of the same mutant) were grown at 28°C, under constant far-red light (FRc; 15 µmol m^{-2} s^{-1}). Two experimental replicates **(a-b)** were performed. Asterisk (*) denotes a significant difference ($p < 0.01$) between WT and *ospif* seedlings according to a one-way ANOVA followed by a Dunnett's multiple comparisons test. For **a-b**, respectively, $14 \leq n \leq 40$ and $17 \leq n \leq 40$.

Given that phyB is the most abundant phytochrome in light grown-seedlings and that it is activated by R and inactivated by FR (Butler et al., 1959; Sharrock & Clack, 2002), we expected R light-grown seedlings to develop similarly to the WT in Wc light while FRc light-grown seedlings are expected to grow coleoptiles similar to those of WT in the dark. As expected, when comparing WT coleoptile length

between the different light conditions, the seedlings grown under Wc light displayed either similar or slightly shorter coleoptile length than those grown under Rc light. The coleoptiles of seedlings grown under FRc were much shorter than those of seedlings grown under Dc but always slightly longer than those of Wc or Rc light-grown seedlings (**Figure 3.5**). These results suggest that, under FR light, besides OsphyB, there are other Osphys involved in the regulation of coleoptile elongation and there is enough active Osphy to partially inhibit coleoptile growth. In fact, it is known that OsphyA plays a role in FR-mediated coleoptile development (Takano et al., 2001), thus we hypothesize that OsphyA might interact with OsPIF15 and OsPIF16, since these are the only OsPIFs harboring an active phyA-binding (APA) motif (Cordeiro et al., 2022). If that is proven, the reduction in coleoptile elongation compared to dark could be explained by the interaction between OsphyA and OsPIF15 and/or OsPIF16 under FR light.

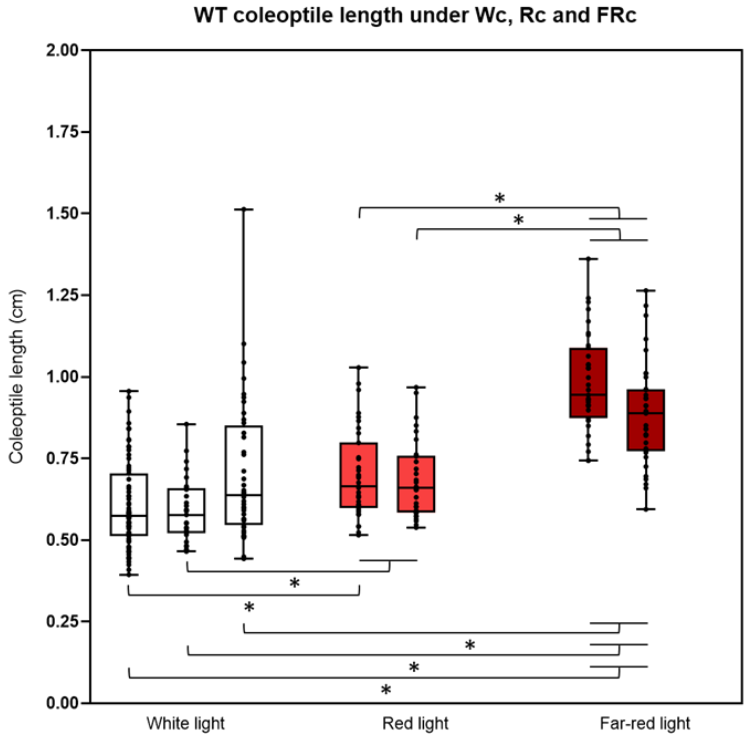

Figure 3.5 Analysis of coleoptile length in WT rice seedlings grown under dark and white, red, and far-red light. Coleoptile length (in cm) was assessed in 9-day-old WT seedlings grown under dark (Dc) and 7-day-old WT seedlings grown under Wc (white), Rc (light red) and FRc (dark red). Asterisk (*) denotes a significant difference ($p < 0.01$) between WT seedlings grown under different light conditions according to a one-way ANOVA followed by a Dunnett's multiple comparisons test.

3.3. OsPIF15 interacts with both OsphyA and OsphyB *in vitro* but OsPIF16 only interacts with OsphyB

The interaction between OsPIF15 and OsphyB has already been reported through both Y2H and BiFC (Xie et al., 2019), and the interaction between OsPIF16 and OsphyB in a Y2H assay has also been described (He et al., 2016). Furthermore, it is known that OsphyB acts as an intermediary in OsPIF15 degradation by light (Xie et al., 2019). Based on these reports, and because phyB is the most prevalent phytochrome in W and R light-grown plants (Sharrock & Clack, 2002; Somers et al., 1991), we expected the WT and *ospif* mutants in the aforementioned coleoptile growth assays to develop the same phenotype under Wc and Rc, which coincides with our results. Under FRc, however, all seedlings developed shorter coleoptiles then the ones in the two previous light conditions, suggesting that OsPIF

regulation under FRc might differ from that under Wc and Rc. Seeing as OsphyA is the dominant FRc light photoreceptor (Takano et al., 2001), and OsPIF15 and OsPIF16 are de only OsPIFs that possess an APA motif (Cordeiro et al., 2022), we decided to investigate the interactions between OsphyA and both OsPIF15 and OsPIF16 through Y2H, using the already reported interactions between these two TFs and OsphyB as positive controls. The interactions between the TFs and phyC, whose function in FRc light perception, although non-essential when phyA is functional, has also been reported (Takano et al., 2001), were tested as well. To do so, OsPIF15 and OsPIF16 and all three rice phytochromes (A to C) were used as both preys (in fusion with the GAL4 activation domain (AD)) and baits (in fusion with the GAL4 binding domain (BD)). In agreement with the aforementioned studies, dot-spotting in SD-L-T-H-A revealed that, when used as preys, OsPIF15 and OsPIF16 both interact with phytochrome B (**Figure 3.6** and **Figure 3.7**). Additionally, we observed that OsphyA interacts with OsPIF15 fused with the GAL4 AD, but not with OsPIF16. The interactions between each OsPIF or Osphy and the empty vectors (ev) were also tested as negative controls, and both OsPIF15 and OsPIF16 showed leaky expression when used as baits, while OsPhyC exhibited leaky expression when employed as prey. As bHLH TFs, OsPIF15 and OsPIF16 may bind to DNA as both homo- and heterodimers, and the homodimerization of OsPIF15 has already been reported (Xie et al., 2019). However, the assessment of the formation of homo- and heterodimers between OsPIF15 and OsPIF16, as well as the interactions between Osphys fused to the GAL4 AD and OsPIF15 or OsPIF16 fused to the GAL4 BD domain, were both hindered by the occurrence of leaky expression. Hence, another technique, such as BiFC, will be required to, not only validate the interactions that have already been reported in other studies and the ones that we detected, but also re-test the interactions that were compromised by the occurrence of leaky expression.

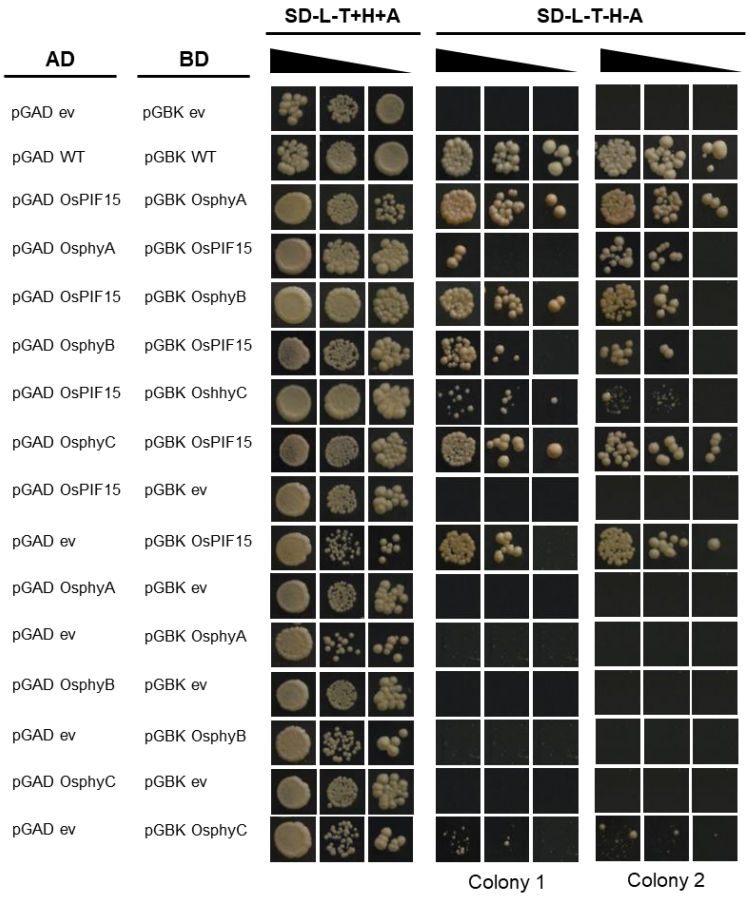

Figure 3.6 *In vitro* analysis of the interactions between OsPIF15 and Osphys using the yeast two-hybrid system. Yeast colonies transformed with the bait (pGBK) and prey (pGAD) plasmids, indicated as BD and AD, respectively, were resuspended in SD medium and serially diluted to 1:10 and 1:100. Each cell culture was dot-spotted in plates containing medium lacking leucine and tryptophan (SD-L-T+H+A; control plate) and selective medium lacking leucine, tryptophan, histidine, and adenine (SD-L-T-H-A; test plate). The pGAD WT/pGBK WT pair (Clontech, California, USA) was used as positive control and pGAD ev/pGBK ev served as negative control. The width of the black triangles indicates 10-fold serial dilutions (1:1, 1:10, 1:100). Colony 1 and colony 2 arise from two independent yeast transformations.

Figure 3.7 *In vitro* analysis of the interactions between OsPIF16 and Osphys using the yeast two-hybrid system. Yeast colonies transformed with the bait (pGBK) and prey (pGAD) plasmids, indicated as BD and AD, respectively, were resuspended in SD medium and serially diluted to 1:10 and 1:100. Each cell culture was dot-spotted in plates containing medium lacking leucine and tryptophan (SD-L-T+H+A; control plate) and selective medium lacking leucine, tryptophan, histidine, and adenine (SD-L-T-H-A; test plate). The pGAD WT/pGBK WT pair (Clontech, California, USA) was used as positive control and pGAD ev/pGBK ev served as negative control. The width of the black triangles indicates 10-fold serial dilutions (1:1, 1:10, 1:100). Colony 1 and colony 2 arise from two independent yeast transformations.

3.4. OsPIF15 and OsPIF16 interact with each other *in planta*

At this time, we have not tested through Bimolecular Fluorescence Complementation (BiFC) all the OsPIF-Osphy interactions that were analyzed by Y2H. Given some technical obstacles and time constraints, we could only obtain preliminary BiFC results for the interactions between OsPIF15 and OsPIF16 *in planta*. In this fluorescence-based approach, two halves of a fluorescent protein (YFP) are fused to each of the two proteins of interest, forming two individual non-fluorescent fusion proteins. Then, if the proteins of interest interact, fluorescence is restored. In this assay, the coding regions of *OsPIF15* and *OsPIF16*, individually cloned in both pYFN^{C}43 and YFP^{N}43, were introduced into the *A. tumefaciens* strain EHA105. The resulting cell cultures were then infiltrated into *Nicotiana benthamiana* leaves, from which leaf samples were collected and visualized under a fluorescence microscope. Fluorescence was detected within the nuclei of *N. benthamiana* cells when YFP^{N}43::OsPIF15 and YFP^{C}43::OsPIF16, YFP^{N}43::OsPIF16 and YFP^{C}43::OsPIF15, YFP^{N}43::OsPIF15 and YFP^{C}43::OsPIF15, as well as YFP^{N}43::OsPIF16 and YFP^{C}43::OsPIF16 were tested (**Figure 3.8**), suggesting that these OsPIFs can form both homo- and heterodimers in the nuclei of *N. benthamiana* cells. However, given the preliminary nature of this experiment, not all interactions were tested at the same time and imaged using the same exposure time, with the putative homo- and heterodimerization of OsPIF15 and OsPIF16 being tested concurrently and captured at an exposure time of 100 ms, while

the interactions between each OsPIF and the empty vectors were tested on a different experiment and images were captured with an exposure time of 120 ms, hindering fluorescence analysis. Moreover, the negative control showed a weaker fluorescent signal than some of the interactions between OsPIFs and the empty vectors, rendering it inadequate to be used for the definition of the fluorescence threshold of the assay. Instead of the empty vectors, using OsPIFs that do not interact with OsPIF15 and OsPIF16 or other TFs belonging to the bHLH family as negative controls would be more advisable. Evidently, optimization of the current protocol will be required to further test the interactions between OsPIF15 and OsPIF16.

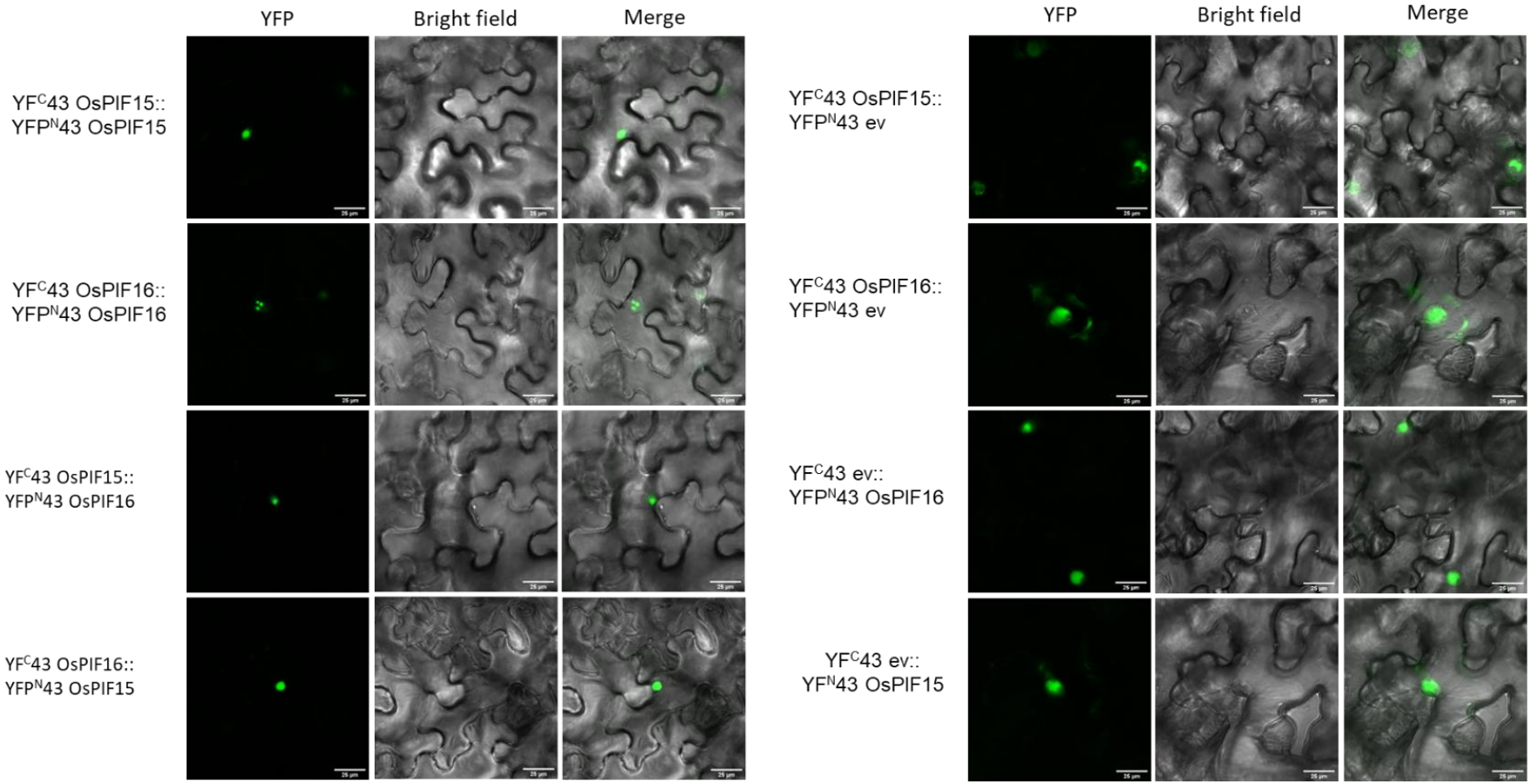

Figure 3.8 Bimolecular Fluorescence Complementation analysis of the protein-protein interactions between OsPIF15 and OsPIF16 *in planta*. YFP^N43::OsPIF15, YFP^C43::OsPIF16, YFP^N43::OsPIF16, YFP^C43::OsPIF15 and the respective empty vectors (ev) were combined as indicated and transiently expressed in *Nicotiana benthamiana* leaf epidermal cells. From left to right: fluorescence microscopy (YFP); bright field microscopy; merged image. Scale bars, 25 µm..

3.5. OsPIF16 is degraded by light in a OsphyB-dependent manner

In Arabidopsis, upon light exposure, phys are activated and migrate into the nucleus, where their interaction with PIFs can lead to the phosphorylation, ubiquitination and proteasome-dependent degradation of these TFs or inhibit their ability to bind to DNA, affecting the transcriptional activation of their target genes and shifting the seedling's developmental program from skoto- to photomorphogenesis (Favero, 2020). In rice, the molecular mechanisms behind the light signaling network that regulates seedling development are still poorly understood. However, it has been reported that OsphyB interacts directly with OsPIF15 under W light, leading to degradation of the latter in a partially OsphyB-dependent manner (Xie et al., 2019). Considering the interaction between OsPIF16 and OsphyB previously identified in our studies, we wondered if, upon light irradiation, OsPIF16 was degraded or sequestered. To assess this, we first tested an antibody that was raised for the full-length sequence of OsPIF16, using samples collected from WT and different *ospif* mutant seedlings grown under constant dark for 8 days (the *ospif12* mutant was not used because it was unavailable at the time). Analysis of the presence of OsPIF16 in *ospif* mutants and WT by Western blotting showed that a band between 63 and 75 kDa was detected in all mutants and WT grown under dark, except for the *ospif16* line (**Figure 3.9 a**). This result confirms that this antibody is specific for OsPIF16 and can be further used to analyze endogenous OsPIF16 levels. Thus, we tested the effect of 24h of continuous white light exposure on the stability of OsPIF16 in WT dark-grown rice plants and found that the OsPIF16 band disappeared when the plant was exposed to constant white light for 24h (**Figure 3.9 b**). To further understand the kinetics of this degradation and if OsPIF16 light-dependent regulation of coleoptile growth is mediated by OsphyB, we performed another assay using 8-day-old etiolated WT and *osphyB-1* mutant seedlings, exposed to white light for 30 min, 1h, 3h, 6h or 9h. In **Figure 3.9 c**, we can observe that, once WT seedlings were exposed to white light, the amount of OsPIF16 that was accumulated in the dark quickly decreased, as evidenced by the very faded OsPIF16 band at 30 min of light exposure. As the time of light exposure increased, OsPIF16 continued to decline until it became undetectable at 6h of light exposure. In the *osphyB-1* mutant there was also a quick degradation of OsPIF16 from 0h to 30 min of light exposure, but the amount of OsPIF16 increased after 3h of light exposure and OsPIF16 was still present at 6h of light exposure, only becoming undetectable at 9h of light exposure (**Figure 3.9 d)**. These results indicate that the degradation of OsPIF16 by white light is dependent on OsphyB, but other players may be responsible for the initial degradation of OsPIF16 until 1h of light exposure and after 6h. Since an antibody specific for OsPIF15 was not available at the lab, we did not test OsPIF15 degradation by light. However, the OsphyB-mediated degradation of OsPIF15 by light has already been described (Xie et al., 2019). In that study, OsPIF15 accumulation in dark-grown WT seedlings rapidly decreased after 30 min of light exposure and it continued declining gradually as the time of exposure to light increased. In *phyB-1* mutants, there was a quick OsPIF15 degradation in the first 1h of light exposure, but the amount of OsPIF15 did not decline as the time of exposure increased and OsPIF15 was still detected at 9h of light exposure, contrary to what we observed for OsPIF16. Altogether, OsPIF15 and OsPIF16 degradation by light is partially dependent on phyB.

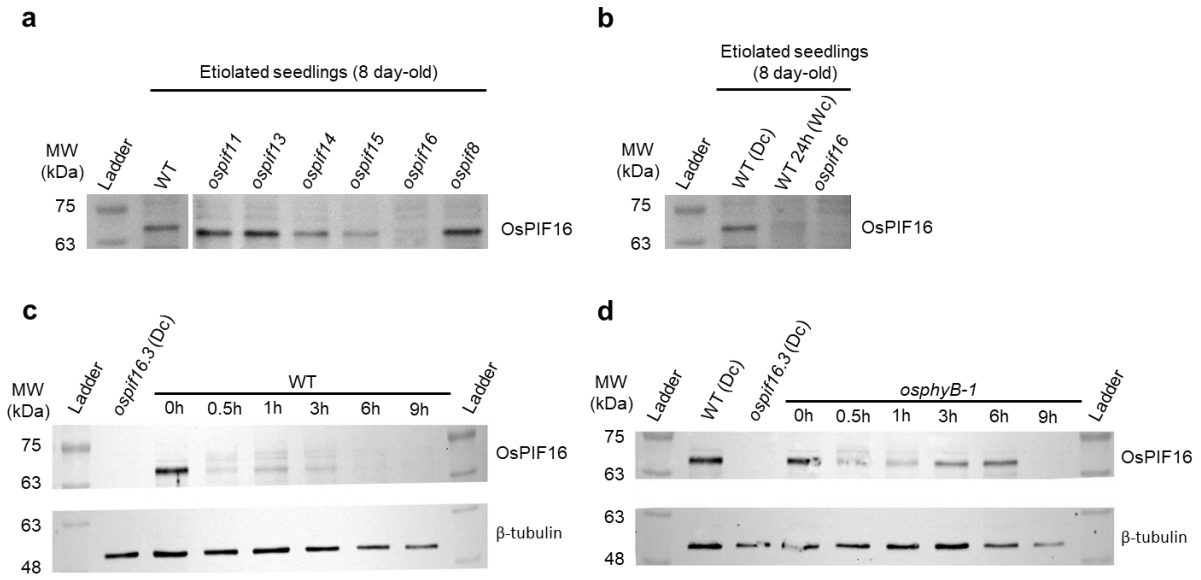

Figure 3.9 Analysis of OsPIF16 stability under white light by Western blotting. (a) Detection of OsPIF16 in the aerial part of 8-day-old etiolated WT and *ospif* mutants by Western blotting. **(b)** Analysis of the effect of 24h of continuous white light exposure on the stability of OsPIF16. Western blots showing OsPIF16 degradation upon increasing exposure to white light: 8-day-old etiolated WT **(c)** and *osphyB-1* **(d)** rice seedlings were transferred to white light for the indicated times. A sample from a dark-grown *ospif16* mutant was used as negative control. Anti-β-tubulin was used as sample loading control.

3.6. Rice *calli* were successfully transformed to overexpress OsPIF15 or OsPIF16

To further unveil the mechanisms by which OsPIF15 and OsPIF16 regulate plant development, we transformed rice *calli* to produce transgenic plants overexpressing either OsPIF15 or OsPIF16 in fusion with a Myc tag under the control of the Zm*Ubi-1* promotor (**Figure 3.10**). The resulting transgenic rice lines will allow us to analyze OsPIF15 and OsPIF16 degradation by different types of light mediated by phytochromes, study protein-protein interactions involving OsPIF15 and OsPIF16, and identify targets genes of these TFs. We performed 9 rounds of transformations for each construct, with only 3 rounds of each construct regenerating plants. In the first rounds of transformation, the *calli* were infected with agrobacterium and transferred directly to CCMS for co-cultivation, with a considerable part of the *calli* being discarded before reaching the selection steps, due to agrobacterium overgrowth. After decreasing the OD_{600} of the agrobacterium suspensions used for transformation in some unsuccessful attempts to reduce agrobacterium overgrowth, we started using filter paper on top of the CCMS plates for the first time during the B017 and B018 transformations. Seeing as these transformations and the following proved to be successful, the previous lack of success could have, indeed, been due to agrobacterium overgrowth hindering co-cultivation of the *calli*. As described in **Table 1**, we obtained a total of 39 plants transformed with the construction to overexpress OsPIF15 and 23 plants transformed with the construction to overexpress OsPIF16, regenerated from 11 and 5 different *calli*, respectively. The latter values represent the minimum number of plant lines produced to overexpress OsPIF15 and OsPIF16, respectively. Depending on the number of insertions of the constructs in each plant, which needs to be determined by Southern blotting, the number of regenerated independent plant lines can be higher. The regenerated plants were transferred to soil. To confirm that these plants were actually transformed and

that their regeneration was not due to an insufficient hygromycin concentration but to the presence of the hygromycin resistance selection marker, a PCR for the hygromycin phosphotransferase II (*HPTII*) gene was performed. In total, all 61 lines were confirmed to contain the *HPTII* gene in their genomic DNA, meaning that they were successfully transformed with OsPIF15-OX or with OsPIF16-OX (**Table 1**).

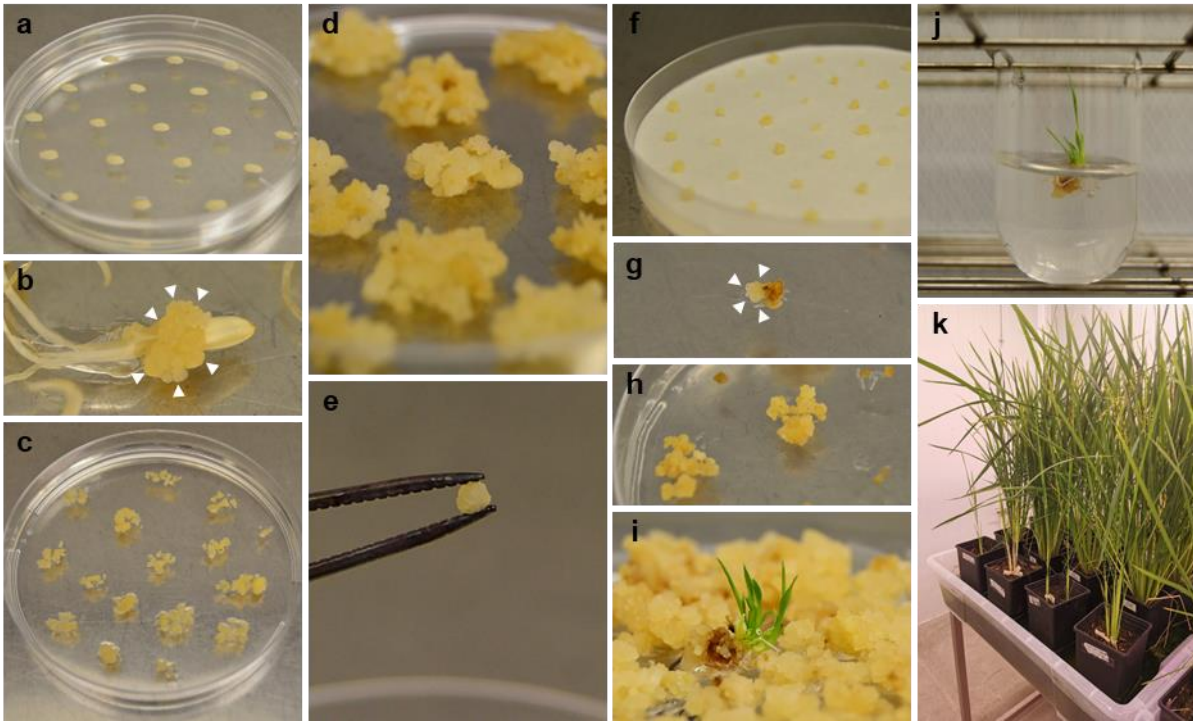

Figure 3.10 Different steps of agrobacterium-mediated transformation of embryogenic *calli* from the Nipponbare rice variety. (a) *Callus* induction from surface-sterilized dehusked seeds on CIM. **(b)** *Scutella* (in between arrowheads) generated from mature rice seeds after 14 days on CIM. **(c)** *Scutella* on fresh CIM, after separation from the seed and root-like structure. **(d)** Actively proliferating scutella with putatively embryogenic *calli.* **(e)** Putatively embryogenic *callus* isolated from *scutella* to be used for transformation. **(f)** Putatively embryogenic *calli* on filter paper placed on top of a CCMS plate after agrobacterium-mediated transformation. **(g)** Co-culture of agrobacterium and rice embryogenic *callus* on SM. Arrowheads indicate the actively growing *callus* tissue next to dying hygromycin-sensitive tissue. **(h)** Proliferation of selected hygromycin-resistant *calli* on EIM. **(i)** Shoot regeneration of putatively transgenic lines on RM from hygromycin-resistant *calli*. **(j)** Rooting and growth of putatively transgenic plantlets on PDM. **(k)** Transgenic plants growing on soil in a transgenic growth chamber.

Table 1. Outcome of rice transformations to generate transgenic plants overexpressing OsPIF15 or OsPIF16.

Transformation	Construction	*Calli* that regenerated cells resistant to 100 mg//L hygromycin	# regenerated plants resistant to 100 mg/L hygromycin	# PCR-positive events
B006	OsPIF15-OX	B006_1	9	9
B017	OsPIF15-OX	B017_1	2	2
B017	OsPIF15-OX	B017_2	3	3
B020	OsPIF15-OX	B020_1	2	2
B020	OsPIF15-OX	B020_3	2	2
B020	OsPIF15-OX	B020_4	4	4
B020	OsPIF15-OX	B020_5	1	1
B020	OsPIF15-OX	B020_6	4	4
B020	OsPIF15-OX	B020_7	5	5
B020	OsPIF15-OX	B020_8	2	2
B020	OsPIF15-OX	B020_9	5	5
Total		11	39	39
B012	OsPIF16-OX	B006_3	5	5
B018	OsPIF16-OX	B018_1	4	4
B018	OsPIF16-OX	B018_2	5	5
B021	OsPIF16-OX	B021_1	7	7
B021	OsPIF16-OX	B021_3	2	2
Total		5	23	23

4. Conclusions and future perspectives

The main aim of this investigation was to unravel the regulatory mechanisms underlying the inhibition of coleoptile growth under dark in *ospif15* and *ospif16* mutants by identifying the protein interactors of OsPIF15 and OsPIF16, determining the role of these TFs in the regulation of rice coleoptile growth under different light conditions and analyzing their protein stability in response to such light conditions in a phytochrome-dependent way. Firstly, our results show that OsPIF15 and OsPIF16 are indeed the main regulators of rice coleoptile growth. These TFs seem to function in a synergistic manner to regulate rice coleoptile development under dark, possibly forming homo- and heterodimers and OsPIF15 is likely to be the major player in this process. Since other *ospif* mutants also developed significantly different from the WT, we cannot exclude the possibility that other OsPIFs may also be involved in the regulation of coleoptile growth under dark. Thus, it would be useful to produce double mutants lacking either OsPIF15 or OsPIF16 and another OsPIF, particularly OsPIF11, which has already been shown to be involved in the regulation of the coleoptile growth (Y. Li et al., 2022).Triple mutants lacking both OsPIF15 and OsPIF16 and another OsPIF would also help to better understand the function of these additional OsPIFs in coleoptile development. Additionally, given that the interaction between rice cryptochromes and PIFs has already been reported to regulate hypocotyl elongation in Arabidopsis (D. Ma et al., 2015; Pedmale et al., 2016), performing coleoptile growth assays using the *ospif* mutants under blue light would allow us to understand if the putative interaction between OsPIF15 or OsPIF16 and the rice cryptochromes also influences coleoptile elongation under blue light. Our Y2H studies showed a clear interaction between OsPIF15 and phyA. This is in agreement with the results by Takano and colaborators, 2005, who showed that OsphyA plays an important role in the regulation of coleoptile growth. We hypothesize that under dark, when Osphys are inactive, OsPIFs are free to bind to their DNA targets, inducing skotomorphogensis and, upon red light exposure, OsphyB is activated, inducing OsPIF16 and OsPIF15 degradation and enabling photomorphogenesis. Under FR light, phyB is inactivated but phyA is activated and its interaction with OsPIF15 leads to OsPIF15 inactivation/degradation, thus inhibiting coleoptile elongation. Again, this is in agreement with the results obtained by Takano et al., 2005, but the interactions between OsPIF15 and OsPIF16 and OsphyA need to be validated *in planta* through BiFC. The interaction between OSPIF15 and OsPIF16 also needs to be investigated using an optimized BiFC protocol. Another option to test these interactions is to perform immunoprecipitation (IP) in the OsPIF15-OX and OsPIF16-OX plants that we have produced, using the anti-Myc tag antibody. This technique could be followed by mass spectrometry (IP-MS). Alternatively, after IP of the OsPIF15, we could perform a Western blot analysis (IP-WB), using the anti-OsPIF16 antibody, to assess if OsPIF16 interacts with OsPIF15. Regarding the degradation assays, it would be very interesting to analyze OsPIF15 degradation by W and R light in a phyA-dependent manner, using *phyA*$^{-1}$ mutant plants and an anti-OsPIF15 antibody. Since this antibody is not available, we can analyze OsPIF15 degradation by FR light using the OsPIF15-OX transgenic plants. Other light conditions could also be tested. The OsPIF15-OX and OsPIF16-OX plants that we developed still need to be characterized regarding their gene expression and protein levels. Once that is done, they will be ready to be used in various assays, such as pulldown assays to test protein-protein interactions, chromatin immunoprecipitation followed by sequencing (ChIP-seq) to identify the DNA targets of OsPIF15 and

OsPIF16, as well as RNA-seq to identify genes differentially expressed in plants overexpressing these TFs. Crossing the results of the two last techniques will increase the chances of identifying target genes for OsPIF15 and OsPIF16. Our results provide new insights into the biological function of OsPIFs and OsphyB regulatory mechanisms in the light regulation of rice seedling development, in particularly coleoptile growth, and, together with the tools generated, are an excellent basis to continue unveiling the regulatory networks underlying rice photo- and skotomorphogenesis.

5. References

Arora, N. K. (2019). Impact of climate change on agriculture production and its sustainable solutions. *Environmental Sustainability*, *2*, 95–96. https://doi.org/10.1007/s42398-019-00078-w

Bae, G., & Choi, G. (2008). Decoding of Light Signals by Plant Phytochromes and Their Interacting Proteins. *Annual Review of Plant Biology*, *59*, 281–311. https://doi.org/10.1146/annurev.arplant.59.032607.092859

Battle, M. W., Vegliani, F., & Jones, M. A. (2020). Shades of green: Untying the knots of green photoperception. *Journal of Experimental Botany*, *71*(19), 5764–5770. https://doi.org/10.1093/jxb/eraa312

Belda-Palazón, B., Ruiz, L., Martí, E., Tárraga, S., Tiburcio, A. F., Culiáñez, F., Farràs, R., Carrasco, P., & Ferrando, A. (2012). Aminopropyltransferases Involved in Polyamine Biosynthesis Localize Preferentially in the Nucleus of Plant Cells. *PLoS ONE*, *7*(10), e46907. https://doi.org/10.1371/journal.pone.0046907

Botto, J. F., Sánchez, R. A., Whitelam, G. C., & Casal, J. J. (1996). Phytochrome A mediates the promotion of seed germination by very low fluences of light and canopy shade light in arabidopsis. *Plant Physiology*, *110*(2), 439–444. https://doi.org/10.1104/pp.110.2.439

Bouly, J., Schleicher, E., Dionisio-sese, M., Vandenbussche, F., Straeten, D. Van Der, Bakrim, N., Meier, S., Batschauer, A., Galland, P., Bittl, R., & Ahmad, M. (2007). Cryptochrome Blue Light Photoreceptors Are Activated through Interconversion of Flavin Redox States. *Journal of Biological Chemistry*, *282*(13), 9383–9391. https://doi.org/10.1074/jbc.M609842200

Butler, W. L., Norris, K. H., Siegelman, H. W., & Hendricks, S. B. (1959). Detection, Assay, and Preliminary Purification of the Pigment Controlling Photoresponsive Development of Plants. *Proc Natl Acad Sci U S A*, *45*(12), 1703–1708. https://doi.org/10.1073/pnas.45.12.1703

Chen, M., & Chory, J. (2011). Phytochrome signaling mechanisms and the control of plant development. *Trends in Cell Biology*, *21*(11), 664–671. https://doi.org/10.1016/j.tcb.2011.07.002

Chory, J. (1993). Out of darkness: Mutants reveal pathways controlling light-regulated development in plants. *Trends in Genetics*, *9*(5), 167–172. https://doi.org/10.1016/0168-9525(93)90163-c

Christie, J. M. (2007). Phototropin blue-light receptors. *Annual Review of Plant Biology*, *58*, 21–45. https://doi.org/10.1146/annurev.arplant.58.032806.103951

Christie, J. M., Arvai, A. S., Baxter, K. J., Heilmann, M., Pratt, A. J., O'Hara, A., Kelly, S. M., Hothorn, M., Smith, B. O., Hitomi, K., Jenkins, G. I., & Getzoff, E. D. (2012). Plant UVR8 Photoreceptor Senses UV-B by Tryptophan- Mediated Disruption of Cross-Dimer Salt Bridges. *Science*, *335*(6075), 1492–1496. https://doi.org/10.1126/science.1218091

Clack, T., Mathews, S., & Sharrock, R. A. (1994). The phytochrome apoprotein family in *Arabidopsis* is encoded by five genes: the sequences and expression of *PHYD* and *PHYE*. *Plant Molecular Biology*, *25*(3), 413–427. https://doi.org/10.1007/BF00043870

Cordeiro, A. M., Andrade, L., Monteiro, C. C., Leitão, G., Wigge, P. A., & Saibo, N. J. M. (2022). PHYTOCHROME-INTERACTING FACTORS: a promising tool to improve crop productivity. *Journal of Experimental Botany*, *73*(12), 3881–3897. https://doi.org/10.1093/jxb/erac142

Cordeiro, A. M., Figueiredo, D. D., Tepperman, J., Rita, A., Lourenço, T., Abreu, I. A., Ouwerkerk, P. B. F., Quail, P. H., Oliveira, M. M., & Saibo, N. J. M. (2016). Rice phytochrome-interacting factor protein OsPIF14 represses *OsDREB1B* gene expression through an extended N-box and interacts preferentially with the active form of phytochrome B. *Biochimica et Biophysica Acta* , *1859*(2), 393–404. https://doi.org/10.1016/j.bbagrm.2015.12.008

Demarsy, E., & Fankhauser, C. (2009). Higher plants use LOV to perceive blue light. *Current Opinion in Plant Biology*, *12*(1), 69–74. https://doi.org/10.1016/j.pbi.2008.09.002

Exner, V., Alexandre, C., Rosenfeldt, G., Alfarano, P., Nater, M., Caflisch, A., Gruissem, W., Batschauer, A., & Hennig, L. (2010). A Gain-of-Function Mutation of Arabidopsis CRYPTOCHROME1 Promotes Flowering. *Plant Physiology*, *154*(4), 1633–1645. https://doi.org/10.1104/pp.110.160895

Fankhauser, C., & Chory, J. (1997). Light Control of Plant Development. *Annual Review of Cell and Developmental Biology2*, *13*, 203–229. https://doi.org/10.1146/annurev.cellbio.13.1.203

Favero, D. S. (2020). Mechanisms regulating PIF transcription factor activity at the protein level. *Physiologia Plantarum*, *169*(3), 325–335. https://doi.org/10.1111/ppl.13075

Fernández, María B., Tossi, V., Lamattina, L., & Cassia, R. (2016). A Comprehensive Phylogeny Reveals Functional Conservation of the UV-B photoreceptor UVR8 from Green Algae to Higher Plants. *Frontiers in Plant Science*, *7*, 1–6. https://doi.org/10.3389/fpls.2016.01698

Fernández, María Belén, Lamattina, L., & Cassia, R. (2020). Functional analysis of the UVR8 photoreceptor from the monocotyledonous Zea mays. *Plant Growth Regulation*, *92*, 307–318. https://doi.org/10.1007/s10725-020-00639-8

Finch-Savage, W. E., & Bassel, G. W. (2016). Seed vigour and crop establishment: Extending performance beyond adaptation. *Journal of Experimental Botany*, *67*(3), 567–591. https://doi.org/10.1093/jxb/erv490

Flint, L. H., & McAlister, E. D. (1935). Wave lengths of radiation in the visible spectrum inhibiting the germination of light-sensitive lettuce seed. *Smithsonian Miscellaneous Collections*, *94*(5), 1–11.

Flint, L. H., & McAlister, E. D. (1937). Wave lengths of radiation in the visible spectrum promoting the germination of light-sensitive lettuce seed (with one plate). *Smithsonian Miscellaneous Collections*, *96*(2), 1–8.

Food and Agriculture Organization of the United Nations (FAO). (2016). *Climate change and food security: Risks and responses*. https://www.fao.org/3/i5188e/i5188e.pdf

Food and Agriculture Organization of the United Nations (FAO) and International Institute for Applied Systems Analysis (IIASA). (2007*) Mapping biophysical factors that influence agricultural*

production and rural vulnerability. https://www.fao.org/3/a1075e/a1075e.pdf

Fujimori, T., Yamashino, T., Kato, T., & Mizuno, T. (2004). Circadian-Controlled Basic/Helix-Loop-Helix Factor, PIL6, Implicated in Light-Signal Transduction in *Arabidopsis thaliana*. *Plant & Cell Pysiology*, *45*(8), 1078–1086. https://doi.org/10.1093/pcp/pch124

Gnanamanickam, S., Kavitha, P. V., Babujee, L., & Brindha Priyadarisini, V. (2002). Biological Control of Rice Diseases. In *Biological Control of Crop Diseases* (Springer). https://doi.org/10.1007/978-90-481-2465-7

Gommers, C. M. M., & Monte, E. (2018). Seedling establishment: A dimmer switch-regulated process between dark and light signaling. *Plant Physiology*, *176*(2), 1061–1074. https://doi.org/10.1104/pp.17.01460

Guo, H., Yang, H., Mockler, T. C., & Lin, C. (1998). Regulation of flowering time by *Arabidopsis* photoreceptors. *Science*, *279*(5355), 1360–1363. https://doi.org/10.1126/science.279.5355.1360

He, Y., Li, Y., Cui, L., Xie, L., Zheng, C., Zhou, G., Zhou, J., & Xie, X. (2016). Phytochrome B Negatively Affects Cold Tolerance by Regulating *OsDREB1* Gene Expression through Phytochrome Interacting Factor-Like Protein OsPIL16 in Rice. *Frontiers in Plant Science*, *7*, 1–12. https://doi.org/10.3389/fpls.2016.01963

Hiei, Y., Ohta, S., Komari, T., & Kumashiro, T. (1994). Efficient transformation of rice (*Oryza sativa* L.) mediated by *Agrobacterium* and sequence analysis of the boundaries of the T-DNA. *The Plant Journal*, *6*(2), 271–282. https://doi.org/10.1046/j.1365-313x.1994.6020271.x

Hiltbrunner, A., Viczián, A., Bury, E., Tscheuschler, A., Kircher, S., Tóth, R., Honsberger, A., Nagy, F., Fankhauser, C., & Schäfer, E. (2005). Nuclear accumulation of the phytochrome A photoreceptor requires FHY1. *Current Biology*, *15*(23), 2125–2130. https://doi.org/10.1016/j.cub.2005.10.042

Hirose, F., Shinomura, T., Tanabata, T., Shimada, H., & Takano, M. (2006). Involvement of Rice Cryptochromes in De-etiolation Responses and Flowering. *Plant and Cell Physiology*, *47*(7), 915–925. https://doi.org/10.1093/pcp/pcj064

Huq, E., Al-Sady, B., Hudson, M., Kim, C., Apel, K., & Quail, P. H. (2004). Phytochrome-interacting factor 1 is a critical bHLH: Regulator of chlorophyll biosynthesis. *Science*, *305*(5692), 1937–1941. https://doi.org/10.1126/science.1099728

Huq, E., Al-Sady, B., & Quail, P. H. (2003). Nuclear translocation of the photoreceptor phytochrome B is necessary for its biological function in seedling photomorphogenesis. *Plant Journal*, *35*(5), 660–664. https://doi.org/10.1046/j.1365-313X.2003.01836.x

Huq, E., & Quail, P. H. (2002). PIF4, a phytochrome-interacting bHLH factor, functions as a negative regulator of phytochrome B signaling in *Arabidopsis*. *The EMBO Journal*, *21*(10), 2441–2450. https://doi.org/10.1093/emboj/21.10.2441

Idris, M., Seo, N., Jiang, L., Kiyota, S., Hidema, J., & Iino, M. (2020). UV-B signalling in rice: Response

identification, gene expression profiling and mutant isolation. *Plant Cell and Environment*, *44*(5), 1468–1485. https://doi.org/10.1111/pce.13988

Jenkins, G. I. (2014). The UV-B photoreceptor UVR8: From structure to physiology. *The Plant Cell*, *26*(1), 21–37. https://doi.org/10.1105/tpc.113.119446

Ji, X., Du, Y., Li, F., Sun, H., Zhang, J., Li, J., Peng, T., Xin, Z., & Zhao, Q. (2019). The basic helix-loop-helix transcription factor, OsPIL15, regulates grain size via directly targeting a purine permease gene *OsPUP7* in rice. *Plant Biotechnology Journal*, *17*(8), 1527–1537. https://doi.org/10.1111/pbi.13075

Jiao, Y., Lau, O. S., & Deng, X. W. (2007). Light-regulated transcriptional networks in higher plants. *Nature Reviews Genetics*, *8*(3), 217–230. https://doi.org/10.1038/nrg2049

Johkan, M., Shoji, K., Goto, F., Hahida, S., & Yoshihara, T. (2012). Effect of green light wavelength and intensity on photomorphogenesis and photosynthesis in *Lactuca sativa*. *Environmental and Experimental Botany*, *75*, 128–133. https://doi.org/10.1016/j.envexpbot.2011.08.010

Jones, A. M., & Edgerton, M. D. (1994). The anatomy of phytochrome, a unique photoreceptor in plants. *Seminars in Cell Biology*, *5*(5), 295–302. https://doi.org/10.1006/scel.1994.1036

Josse, E.-M., & Halliday, K. J. (2008). Skotomorphogenesis: The Dark Side of Light Signalling. *Current Biology*, *18*(24), R1144–R1146. https://doi.org/10.1016/j.cub.2008.10.034

Kagawa, T. (2003). The phototropin family as photoreceptors for blue light-induced chloroplast relocation. *Journal of Plant Research*, *116*(1), 77–82. https://doi.org/10.1007/s10265-002-0072-4

Kami, C., Lorrain, S., Hornitschek, P., & Fankhauser, C. (2010). Light-regulated plant growth and development. *Current Topics in Developmental Biology*, *91*, 29–66. https://doi.org/10.1016/S0070-2153(10)91002-8

Kanegae, H., Tahir, M., Savazzini, F., Yamamoto, K., Yano, M., Sasaki, T., Kanegae, T., Wada, M., & Takano, M. (2000). Rice NPH1 homologues, OsNPH1a and OsNPH1b, are differently photoregulated. *Plant and Cell Physiology*, *41*(4), 415–423. https://doi.org/10.1093/pcp/41.4.415

Kay, S. A. (1997). PAS, present, and future: Clues to the origins of circadian clocks. *Science*, *276*(5313), 753–754. https://doi.org/10.1126/science.276.5313.753

Khadka, K., Kaviani, M., Raizada, M. N., & Navabi, A. (2021). Phenotyping and Identification of Reduced Height (*Rht*) Alleles (*Rht-B1b* and *Rht-D1b*) in a Nepali Spring Wheat (*Triticum aestivum* L.) Diversity Panel to Enable Seedling Vigor Selection. *Agronomy*, *11*(12). https://doi.org/10.3390/agronomy11122412

Khanna, R., Huq, E., Kikis, E. A., Al-Sady, B., Lanzatella, C., & Quail, P. H. (2004). A novel molecular recognition motif necessary for targeting photoactivated phytochrome signaling to specific basic helix-loop-helix transcription factors. *The Plant Cell*, *16*(11), 3033–3044. https://doi.org/10.1105/tpc.104.025643

Kinoshita, T., Doi, M., Suetsugu, N., Kagawa, T., Wada, M., & Shimazaki, K. (2001). phot1 and phot2 mediate blue light regulation of stomatal opening. *Nature*, *414*(6864), 656–660. https://doi.org/10.1038/414656a

Kiontke, S., Göbel, T., Brych, A., & Batschauer, A. (2020). DASH-type cryptochromes - Solved and open questions. *Biological Chemistry*, *401*(12), 1487–1493. https://doi.org/10.1515/hsz-2020-0182

Kircher, S., Kozma-Bognar, L., Kim, L., Adam, E., Harter, K., Schäfer, E., & Nagy, F. (1999). Light quality-dependent nuclear import of the plant photoreceptors phytochrome A and B. *The Plant Cell*, *11*(8), 1445–1456. https://doi.org/10.1105/tpc.11.8.1445

Kleine, T., Lockhart, P., & Batschauer, A. (2003). An *Arabidopsis* protein closely related to *Synechocystis* cryptochrome is targeted to organelles. *The Plant Journal*, *35*(1), 93–103. https://doi.org/10.1046/j.1365-313x.2003.01787.x

Klose, C., Viczián, A., Kircher, S., Schäfer, E., & Nagy, F. (2015). Molecular mechanisms for mediating light-dependent nucleo/cytoplasmic partitioning of phytochrome photoreceptors. *New Phytologist*, *206*(3), 965–971. https://doi.org/10.1111/nph.13207

Lagarias, D. M., Wu, S. H., & Lagarias, J. C. (1995). Atypical phytochrome gene structure in the green alga *Mesotaenium caldariorum*. *Plant Molecular Biology*, *29*(6), 1127–1142. https://doi.org/10.1007/BF00020457

Lee, N., & Choi, G. (2017). Phytochrome-interacting factor from Arabidopsis to liverwort. *Current Opinion in Plant Biology*, *35*, 54–60. https://doi.org/10.1016/j.pbi.2016.11.004

Leivar, P., Monte, E., Al-Sady, B., Carle, C., Storer, A., Alonso, J. M., Ecker, J. R., & Quaila, P. H. (2008). The *Arabidopsis* phytochrome-interacting factor PIF7, together with PIF3 and PIF4, regulates responses to prolonged red light by modulating phyB levels. *The Plant Cell*, *20*(2), 337–352. https://doi.org/10.1105/tpc.107.05214

Leivar, P., Monte, E., Oka, Y., Liu, T., Carle, C., Castillon, A., Huq, E., & Quail, P. H. (2008). Multiple Phytochrome-Interacting bHLH Transcription Factors Repress Premature Seedling Photomorphogenesis in Darkness. *Current Biology*, *18*(23), 1815–1823. https://doi.org/10.1016/j.cub.2008.10.058

Li, L., Ljung, K., Breton, G., Schmitz, R. J., Pruneda-paz, J., Cowing-Zitron, C., Cole, B. J., Ivans, L. J., Pedmale, U. V, Jung, H.-S., Ecker, J. R., Kay, S. A., & Chory, J. (2012). Linking photoreceptor excitation to changes in plant architecture. *Genes & Development*, *26*(8), 785–790. https://doi.org/10.1101/gad.187849.112

Li, X., Duan, X., Jiang, H., Sun, Y., Tang, Y., Yuan, Z., Guo, J., Liang, W., Chen, L., Yin, J., Ma, H., Wang, J., & Zhang, D. (2006). Genome-Wide Analysis of Basic/ Helix-Loop-Helix Transcription Factor Family in Rice and Arabidopsis. *Plant Physiology*, *141*(4), 1167–1184. https://doi.org/10.1104/pp.106.080580

Li, Y., Zhang, F., Zheng, C., Zhou, J., Meng, X., Niu, S., Chen, F., Zhang, H., & Xie, X. (2022). Fusion of the SRDX Motif to OsPIL11 or OsPIL16 Causes Rice Constitutively Photomorphogenic Phenotypes In Darkness. *Plant Growth Regulation*, *96*, 157–175. https://doi.org/10.1007/s10725-021-00767-9

Lin, C. (2002). Blue Light Receptors and Signal Transduction. *The Plant Cell*, *14 Suppl*(Suppl), S207–S225. https://doi.org/10.1105/tpc.000646

Lin, C., & Shalitin, D. (2003). Cryptochrome Structure and Signal Transduction. *Annual Review of Plant Biology*, *54*, 469–496. https://doi.org/10.1146/annurev.arplant.54.110901.160901

Lin, C., Yang, H., Guo, H., Mockler, T., Chen, J., & Cashmore, A. R. (1998). Enhancement of blue-light sensitivity of Arabidopsis seedlings by a blue light receptor cryptochrome 2. *Proceedings of the National Academy of Sciences of the United States of America*, *95*(5), 2686–2690. https://doi.org/10.1073/pnas.95.5.2686

Liu, X., Liu, R., Li, Y., Shen, X., Zhong, S., & Shi, H. (2017). EIN3 and PIF3 form an interdependent module that represses chloroplast development in buried seedlings. *The Plant Cell*, *29*(12), 3051–3067. https://doi.org/10.1105/tpc.17.00508

Lorrain, S., Allen, T., Duek, P. D., Whitelam, G. C., & Fankhauser, C. (2008). Phytochrome-mediated inhibition of shade avoidance involves degradation of growth-promoting bHLH transcription factors. *The Plant Journal*, *53*(2), 312–323. https://doi.org/10.1111/j.1365-313X.2007.03341.x

Luo, Q., Lian, H. L., He, S. B., Li, L., Jia, K. P., & Yang, H. Q. (2014). COP1 and phyB Physically Interact with PIL1 to Regulate Its Stability and Photomorphogenic Development in *Arabidopsis*. *The Plant Cell*, *26*(6), 2441–2456. https://doi.org/10.1105/tpc.113.121657

Ma, D., Li, X., Guo, Y., Chu, J., Fang, S., Yan, C., & Noel, J. P. (2015). Cryptochrome 1 interacts with PIF4 to regulate high temperature-mediated hypocotyl elongation in response to blue light. *Proceedings of the National Academy of Sciences If the United States of America*, *113*(1), 224–229. https://doi.org/10.1073/pnas.1511437113

Ma, L., Li, J., Qu, L., Hager, J., Chen, Z., Zhao, H., & Deng, X. W. (2001). Light Control of Arabidopsis Development Entails Coordinated Regulation of Genome Expression and Cellular Pathways. *The Plant Cell*, *13*(12), 2589–2607. https://doi.org/10.1105/tpc.010229

Matchmaker ® Gold Yeast Two-Hybrid System User Manual (Issue 0). (n.d.). Takara Bio USA, Inc.

Mathews, S., & Sharrock, R. A. (1996). The phytochrome gene family in grasses (Poaceae): A phylogeny and evidence that grasses have a subset of the loci found in dicot angiosperms. *Molecular Biology and Evolution*, *13*(8), 1141–1150. https://doi.org/10.1093/oxfordjournals.molbev.a025677

Mo, W., Tang, W., Du, Y., Jing, Y., Bu, Q., & Lin, R. (2020). PHYTOCHROME-INTERACTING FACTOR-LIKE14 and SLENDER RICE1 Interaction Controls Seedling Growth under Salt Stress. *Plant*

Physiology, *184*(1), 506–517. https://doi.org/10.1104/PP.20.00024

Mohr, H. (1962). Primary Effects of Light on Growth. *Annual Review of Plant Physiology*, *13*, 465–488. https://doi.org/10.1146/annurev.pp.13.060162.002341

Munaweera, T. I. K., Jayawardana, N. U., Rajaratnam, R., & Dissanayake, N. (2022). Modern plant biotechnology as a strategy in addressing climate change and attaining food security. *Agriculture & Food Security*, *11*(26), 1–28. https://doi.org/10.1186/s40066-022-00369-2

Nagatani, A., Reed, J. W., & Chory, J. (1993). Isolation and initial characterization of *Arabidopsis* mutants that are deficient in phytochrome A. *Plant Physiology*, *102*(1), 269–277. https://doi.org/10.1104/pp.102.1.269

Nakamura, Y., Kato, T., Yamashino, T., Murakami, M., & Mizuno, T. (2007a). Characterization of a Set of Phytochrome-Interacting Factor-Like bHLH Proteins in *Oryza sativa*. *Bioscience, Biotechnology and Biochemistry*, *71*(5), 1183–1191. https://doi.org/10.1271/bbb.60643

Nakamura, Y., Kato, T., Yamashino, T., Murakami, M., & Mizuno, T. (2007b). Characterization of a Set of Phytochrome-Interacting Factor-Like bHLH Proteins in Oryza sativa. *Bioscience, Biotechnology, and Biochemistry*, *71*(5), 1183–1191. https://doi.org/10.1271/bbb.60643

Ni, M., Tepperman, J. M., & Quail, P. H. (1998). PIF3 , a Phytochrome-Interacting Factor Necessary for Normal Photoinduced Signal Transduction , Is a Novel Basic Helix-Loop-Helix Protein. *Cell*, *95*(5), 657–667. https://doi.org/10.1016/s0092-8674(00)81636-0

Ni, M., Tepperman, J. M., & Quail, P. H. (1999). Binding of phytochrome B to its nuclear signalling partner PIF3 is reversibly induced by light. *Nature*, *400*(6746), 781–784. https://doi.org/10.1038/23500

Oh, E., Kim, J., Park, E., Kim, J.-I., Kang, C., & Choi, G. (2004). PIL5, a phytochrome-interacting basic helix-loop-helix protein, is a key negative regulator of seed germination in *Arabidopsis thaliana*. *The Plant Cell*, *16*(11), 3045–3058. https://doi.org/10.1105/tpc.104.025163

Oh, J., Park, E., Song, K., Bae, G., & Choi, G. (2020). PHYTOCHROME INTERACTING FACTOR8 Inhibits Phytochrome A-Mediated Far-Red Light Responses in Arabidopsis. *The Plant Cell*, *32*(1), 186–205. https://doi.org/10.1105/tpc.19.00515

Parks, B. M., & Quail, P. H. (1993). *hy*8, a new class of arabidopsis long hypocotyl mutants deficient in functional phytochrome A. *The Plant Cell*, *5*(1), 39–48. https://doi.org/10.1105/tpc.5.1.39

Pedmale, U. V, Huang, S. C., Zander, M., Cole, B. J., Hetzel, J., Ljung, K., Reis, P. A. B., Sridevi, P., Nito, K., Nery, J. R., Ecker, J. R., Ecker, J. R., & Chory, J. (2016). Cryptochromes Interact Directly with PIFs to Control Plant Growth in Limiting Blue Light. *Cell*, *164*(1–2), 233–245. https://doi.org/10.1016/j.cell.2015.12.018

Pfeiffer, A., Nagel, M. K., Popp, C., Wüst, F., Bindics, J., Viczián, A., Hiltbrunner, A., Nagy, F., Kunkel, T., & Schäfer, E. (2012). Interaction with plant transcription factors can mediate nuclear import of

phytochrome B. *Proceedings of the National Academy of Sciences of the United States of America*, *109*(15), 5892–5897. https://doi.org/10.1073/pnas.1120764109

Pham, V. N., Kathare, P. K., & Huq, E. (2018). Phytochromes and phytochrome interacting factors. *Plant Physiology*, *176*(2), 1025–1038. https://doi.org/10.1104/pp.17.01384

Pokorny, R., Klar, T., Hennecke, U., Carell, T., Batschauer, A., & Essen, L. O. (2008). Recognition and repair of UV lesions in loop structures of duplex DNA by DASH-type cryptochrome. *Proceedings of the National Academy of Sciences of the United States of America*, *105*(52), 21023–21027. https://doi.org/10.1073/pnas.0805830106

Ponnu, J., & Hoecker, U. (2022). Signaling Mechanisms by Arabidopsis Cryptochromes. *Frontiers in Plant Science*, *13*. https://doi.org/10.3389/fpls.2022.844714

Porter, J. R., Xie, L., Challinor, A. J., Cochrane, K., Howden, S. M., Iqbal, M. M., Lobell, D. B., & Travasso, M. I. (2014). Food security and food production systems. In P. Aggarwal & K. Hakala (Eds.), *Climate Change 2014: Impacts, Adaptation and Vulnerability. Part A: Global and Sectoral Aspects* (pp. 485–533). Cambridge University Press, United Kingdom and New York, NY, USA.

Quail, P. H. (1998). The phytochrome family: dissection of functional roles and signalling pathways among family members. *Philosophical Transactions of the Royal Society of London. Series B, Biological Sciences*, *353*(1374), 1399–1403. https://doi.org/10.1098/rstb.1998.0294

Quail, P. H., Boylan, M. T., Parks, B. M., Short, T. W., Xu, Y., & Wagner, D. (1995). Phytochromes : Photosensory Perception and Signal Transduction. *Science*, *268*(5211), 675–680. https://doi.org/10.1126/science.7732376

Rausenberger, J., Tscheuschler, A., Nordmeier, W., Wüst, F., Timmer, J., Schäfer, E., Fleck, C., & Hiltbrunner, A. (2011). Photoconversion and nuclear trafficking cycles determine phytochrome A's response profile to far-red light. *Cell*, *146*(5), 813–825. https://doi.org/10.1016/j.cell.2011.07.023

Raza, A., Razzaq, A., Mehmood, S. S., Zou, X., Zhang, X., Lv, Y., & Xu, J. (2019). Impact of climate change on crops adaptation and strategies to tackle its outcome: A review. *Plants*, *8*(2), 34. https://doi.org/10.3390/plants8020034

Rizzini, L., Favory, J., Cloix, C., Faggionato, D., Hara, A. O., Kaiserli, E., Baumeister, R., Schäfer, E., Nagy, F., Jenkins, G. I., & Ulm, R. (2011). Perception of UV-B by the *Arabidopsis* UVR8 Protein. *Science*, *332*(6025), 103–106. https://doi.org/10.1126/science.1200660

Sadeghian, S. Y., & Yavari, N. (2004). Effect of water-deficit stress on germination and early seedling growth in sugar beet. *Journal of Agronomy and Crop Science*, *190*(2), 138–144. https://doi.org/10.1111/j.1439-037X.2004.00087.x

Sahoo, K. K., Tripathi, A. K., Pareek, A., Sopory, S. K., & Singla-Pareek, S. L. (2011). An improved protocol for efficient transformation and regeneration of diverse indica rice cultivars. *Plant Methods*, *7*(1). https://doi.org/10.1186/1746-4811-7-49

Sakai, T., Kagawa, T., Kasahara, M., Swartz, T. E., Christie, J. M., Briggs, W. R., Wada, M., & Okada, K. (2001). *Arabidopsis* nph1 and npl1 : Blue light receptors that mediate both phototropism and chloroplast relocation. *Proceedings of the National Academy of Sciences of the United States of America*, *98*(12), 6969–6974. https://doi.org/10.1073/pnas.101137598

Sakamoto, K., & Briggs, W. R. (2002). Cellular and subcellular localization of phototropin 1. *The Plant Cell*, *14*(8), 1723–1735. https://doi.org/10.1105/tpc.003293

Sakamoto, K., & Nagatani, A. (1996). Nuclear localization activity of phytochrome B. *The Plant Journal*, *10*(5), 859–868. https://doi.org/10.1046/j.1365-313x.1996.10050859.x

Sancar, A. (2003). Structure and function of DNA photolyase and cryptochrome blue-light photoreceptors. *Chemical Reviews*, *103*(6), 2203–2237. https://doi.org/10.1021/cr0204348

Sang, Y., Li, Q. H., Rubio, V., Zhang, Y. C., Mao, J., Deng, X. W., & Yang, H. Q. (2005). N-terminal domain-mediated homodimerization is required for photoreceptor activity of Arabidopsis Cryptochrome 1. *The Plant Cell*, *17*(5), 1569–1584. https://doi.org/10.1105/tpc.104.029645

Schäfer, E., & Bowler, C. (2002). Phytochrome-mediated photoperception and signal transduction in higher plants. *EMBO Reports*, *3*(11), 1042–1048. https://doi.org/10.1093/embo-reports/kvf222

Schlichting, C. D. (1986). The Evolution of Phenotypic Plasticity in Plants. *Annual Review of Ecology and Systematics*, *17*, 667–693. https://doi.org/10.1146/annurev.es.17.110186.003315

Shalitin, D., Yang, H., Mockler, T. C., Maymon, M., Guo, H., Whitlam, G. C., & Lin, C. (2002). Regulation of *Arabidopsis* cryptochrome 2 by blue-light- dependent phosphorylation. *Nature*, *417*(6890), 763–767. https://doi.org/10.1038/nature00815

Shalitin, D., Yu, X., Maymon, M., Mockler, T., & Lin, C. (2003). Blue Light – Dependent *in Vivo* and *in Vitro* Phosphorylation of Arabidopsis Cryptochrome 1. *The Plant Cell*, *15*(10), 2421–2429. https://doi.org/10.1105/tpc.013011

Sharrock, R. A., & Clack, T. (2002). Patterns of Expression and Normalized Levels of the Five Arabidopsis Phytochromes 1. *Plant Physiology*, *130*(1), 442–456. https://doi.org/10.1104/pp.005389

Sharrock, R. A., & Clack, T. (2004). Heterodimerization of type II phytochromes in *Arabidopsis*. *Proceedings of the National Academy of Sciences of the United States of America*, *101*(31), 11500–11505. https://doi.org/10.1073/pnas.0404286101

Sheerin, D. J., & Hiltbrunner, A. (2017). Molecular mechanisms and ecological function of far-red light signalling. *Plant, Cell & Environment*, *40*(11), 2509–2529. https://doi.org/10.1111/pce.12915

Shi, H., Lyu, M., Luo, Y., Liu, S., Li, Y., He, H., Wei, N., Deng, X. W., & Zhong, S. (2018). Genome-wide regulation of light-controlled seedling morphogenesis by three families of transcription factors. *Proceedings of the National Academy of Sciences of the United States of America*, *115*(25), 6482–6487. https://doi.org/10.1073/pnas.1803861115

Shi, H., Shen, X., Liu, R., Xue, C., Wei, N., Deng, X. W., & Zhong, S. (2016). The Red Light Receptor Phytochrome B Directly Enhances Substrate-E3 Ligase Interactions to Attenuate Ethylene Responses. *Developmental Cell*, *39*(5), 597–610. https://doi.org/10.1016/j.devcel.2016.10.020

Shinomura, T., Nagatani, A., Hanzawa, H., Kubota, M., Watanabe, M., & Furuya, M. (1996). Action spectra for phytochrome A- and B-specific photoinduction of seed germination in *Arabidopsis thaliana*. *Proceedings of the National Academy of Sciences of the United States of America*, *93*(15), 8129–8133. https://doi.org/10.1073/pnas.93.15.8129

Sineshchekov, V. A. (2023). *Two Distinct Molecular Types of Phytochrome A in Plants : Evidence of Existence and Implications for Functioning*.

Singh, S., Agrawal, S. B., & Agrawal, M. (2015). Role of Light in Plant Development. *International Journal of Plant and Environment*, *1*(1), 43–56. https://doi.org/10.18811/ijpen.v1i1.7113

Smith, H. (1982). Light Quality, Photoperception, and Plant Strategy. *Annual Review of Plant Physiology*, *33*(1), 481–518. https://doi.org/10.1146/annurev.pp.33.060182.002405

Somers, D. E., Devlin, P. F., & Kay, S. A. (1998). Phytochromes and cryptochromes in the entrainment of the *Arabidopsis* circadian clock. *Science*, *282*(5393), 1488–1490. https://doi.org/10.1126/science.282.5393.1488

Somers, D. E., Sharrock, R. A., Teppermaqa, J. M., & Quail, P. H. (1991). The *hy*3 Long Hypocotyl Mutant of Arabidopsis 1 s Deficient in Phytochrome B. *The Plant Cell*, *3*(12), 1263–1274. https://doi.org/10.1105/tpc.3.12.1263

Stevens, N., Seal, C. E., Archibald, S., & Bond, W. (2014). Increasing temperatures can improve seedling establishment in arid-adapted savanna trees. *Oecologia*, *175*(3), 1029–1040. https://doi.org/10.1007/s00442-014-2958-y

Sullivan, J. A., & Deng, X. W. (2003). From seed to seed : the role of photoreceptors in *Arabidopsis* development. *Developmental Biology*, *260*(2), 289–297. https://doi.org/10.1016/s0012-1606(03)00212-4

Takano, M., Inagaki, N., Xie, X., Yuzurihara, N., Hihara, F., Ishizuka, T., Yano, M., Nishimura, M., Miyao, A., Hirochika, H., & Shinomura, T. (2005). Distinct and Cooperative Functions of Phytochromes A , B , and C in the Control of Deetiolation and Flowering in Rice. *The Plant Cell*, *17*(12), 3311–3325. https://doi.org/10.1105/tpc.105.035899.2

Takano, M., Kanegae, H., Shinomura, T., Miyao, A., Hirochika, H., & Furuya, M. (2001). Isolation and Characterization of Rice Phytochrome A Mutants. *The Plant Cell*, *13*(3), 521–534. https://doi.org/10.1105/tpc.13.3.521

Tian, Q. Y., Zhao, Y. P., & Liu, C. J. (2012). Modified yeast-two-hybrid system to identify proteins interacting with the growth factor progranulin. *Journal of Visualized Experiments*, *59*. https://doi.org/10.3791/3562

Todaka, D., Nakashima, K., Maruyama, K., Kidokoro, S., Osakabe, Y., Ito, Y., Matsukura, S., Fujita, Y., Yoshiwara, K., Ohme-Takagi, M., Kojima, M., Sakakibara, H., Shinozaki, K., & Yamaguchi-Shinozaki, K. (2012). Rice phytochrome-interacting factor-like protein OsPIL1 functions as a key regulator of internode elongation and induces a morphological response to drought stress. *Proceedings of the National Academy of Sciences of the United States of America*, *109*(39), 15947–15952. https://doi.org/10.1073/pnas.1207324109

Uçarlı, C. (2020). Effects of Salinity on Seed Germination and Early Seedling Stage. In S. Fahad, S. Saud, Y. Chen, C. Wu, & D. Wang (Eds.), *Abiotic Stress in Plants* (pp. 1–21). IntechOpen. https://doi.org/10.5772/intechopen.91549

United Nations (UN). (2022) *Day of Eight Billion*. https://www.un.org/en/dayof8billion

United Nations Department of Economic and Social Affairs (UN DESA). (2022) *World Population Prospects 2020: Summary of Results.* https://www.un.org/development/desa/pd/sites/www.un.org.development.desa.pd/files/wpp2022_summary_of_results.pdf

Verchot, L. V., Van Noordwijk, M., Kandji, S., Tomich, T., Ong, C., Albrecht, A., Mackensen, J., Bantilan, C., Anupama, K. V., & Palm, C. (2007). Climate change: linking adaptation and mitigation through agroforestry. *Mitigation and Adaptation Strategies for Global Change*, *12*, 901–918. https://doi.org/10.1007/s11027-007-9105-6

Wada, M., Kagawa, T., & Sato, Y. (2003). Chloroplast Movement. *Annual Review of Plant Biology*, *54*, 455–468. https://doi.org/10.1146/annurev.arplant.54.031902.135023

Wang, H. (2005). Signaling Mechanisms of Higher Plant Photoreceptors: A Structure-Function Perspective. *Current Topics in Developmental Biology*, *68*, 227–261. https://doi.org/10.1016/S0070-2153(05)68008-8

Wang, Q., & Lin, C. (2020). Mechanisms of Cryptochrome-Mediated Photoresponses in Plants. *Annual Review of Plant Biology*, *71*, 103–129. https://doi.org/10.1146/annurev-arplant-050718-100300

Whitelam, G. C., & Devlin, P. F. (1997). Roles of different phytochromes in Arabidopsis photomorphogenesis. *Plant, Cell and Environment*, *20*, 752–758. https://doi.org/10.1046/j.1365-3040.1997.d01-100.x

Whitelam, Garry C., Johnson, E., Peng, J., Carol, P., Anderson, M. L., Cowl, J. S., & Harberd, N. P. (1993). Phytochrome a null mutants of arabidopsis display a wild-type phenotype in white light. *The Plant Cell*, *5*(7), 757–768. https://doi.org/10.1105/tpc.5.7.757

Wu, G., & Spalding, E. P. (2007). Separate functions for nuclear and cytoplasmic cryptochrome 1 during photomorphogenesis of *Arabidopsis* seedlings. *Proceedings of the National Academy of Sciences of the United States of America*, *104*(47), 18813–18818. https://doi.org/10.1073/pnas.0705082104

Wu, S., & Lagarias, J. C. (2000). Defining the Bilin Lyase Domain : Lessons from the Extended

Phytochrome. *Biochemistry*, *39*(44), 13487–13495. https://doi.org/10.1021/bi001123z

Xie, C., Zhang, G., An, L., Chen, X., & Fang, R. (2019). Phytochrome - interacting factor - like protein OsPIL15 integrates light and gravitropism to regulate tiller angle in rice. *Planta*, *250*(1), 105–114. https://doi.org/10.1007/s00425-019-03149-8

Yamaguchi, R., Nakamura, M., Mochizuki, N., Kay, S. A., & Nagatani, A. (1999). Light-dependent translocation of a phytochrome B-GFP fusion protein to the nucleus in transgenic Arabidopsis. *The Journal of Cell Biology*, *145*(3), 437–445. https://doi.org/10.1083/jcb.145.3.437

Yamashino, T., Matsushika, A., Fujimori, T., Sato, S., Kato, T., Tabata, S., & Mizuno, T. (2003). A Link between Circadian-Controlled bHLH Factors and the APRR1/TOC1 Quintet in *Arabidopsis thaliana*. *Plant & Cell Pysiology*, *44*(6), 619–629. https://doi.org/10.1093/pcp/pcg078

Young, J. C., Liscum, E., & Hangarter, R. P. (1992). Spectral-dependence of light-inhibited hypocotyl elongation in photomorphogenic mutants of *Arabidopsis*: evidence for a UV-A photosensor. *Planta*, *188*(1), 106–114. https://doi.org/10.1007/BF00198946

Yu, X., Klejnot, J., Zhao, X., Shalitin, D., Maymon, M., Yang, H., Lee, J., Liu, X., Lopez, J., & Lin, C. (2007). *Arabidopsis* Cryptochrome 2 Completes Its Posttranslational Life Cycle in the Nucleus. *The Plant Cell*, *19*(10), 3146–3156. https://doi.org/10.1105/tpc.107.053017

Zhou, J., Liu, Q., Zhang, F., Wang, Y., Zhang, S., Cheng, H., Yan, L., Li, L., Chen, F., & Xie, X. (2014). Overexpression of *OsPIL15* , a phytochrome - interacting factor - like protein gene , represses etiolated seedling growth in rice. *Journal of Integrative Plant Biology*, *56*(4), 373–387. https://doi.org/10.1111/jipb.12137

6. Attachments

Table S1 Composition of the different media used for rice *callus* induction, transformation, and selection and for plant regeneration.

Media composition	CIM	CCMS	CCML	SM	EIM	RM	PDM
N6 Macro I	100 mL/L	-	-	-	-	-	-
N6 Macro II	100 mL/L	-	-	-	-	-	-
R2 Macro I	-	100 mL/L	100 mL/L	100 mL/L	-	-	-
R2 Macro II	-	100 mL/L	100 mL/L	100 mL/L	-	-	-
MS Macro I	-	-	-	-	100 mL/L	100 mL/L	50 mL/L
MS Macro II	-	-	-	-	100 mL/L	100 mL/L	50 mL/L
B5 Vitamins	1 mL/L	-	-	-	-	-	-
R2 Vitamins	-	25 mL/L	25 mL/L	25 mL/L	-	-	-
LS Vitamins	-	-	-	-	10 mL/L	10 mL/L	5 mL/L
R2 FeNa-EDTA	-	10 mL/L	10 mL/L	10 mL/L	-	-	-
MS FeNa-EDTA	10 mL/L	-	-	-	10 mL/L	10 mL/L	5 mL/L
B5 Micro	1 mL/L	-	-	-	-	-	-
R2 Micro	-	1 mL/L	1 mL/L	1 mL/L	-	-	-
MS Micro	-	-	-	-	1 mL/L	1 mL/L	0.5 mL/L
Proline	500 mg/L	-	-	-	-	-	-
Glutamine	500 mg/L	-	-	-	-	-	-
CEH	300 mg/L	-	-	-	-	-	-
2,4-D	2.5 mg/L	2.5 mg/L	2.5 mg/L	2.5 mg/L	2.5 mg/L	-	-
Glucose	-	10 g/L	10 g/L	-	-	-	-
Sucrose	30 g/L	-	-	30 g/L	30 g/L	40 g/L	10 g/L
Gelrite	2.5 g/L	7g/L	-	7g/L	7g/L	7g/L	2.5 g/L
Acetosyringone	-	1 mL/L	-	-	-	-	-
Cefotaxime	-	-	-	1 mL/L	1 mL/L	1 mL/L	-
Vancomycin	-	-	-	1 mL/L	1 mL/L	1 mL/L	-
Hygromycin	-	-	-	1 mL/L	2 mL/L	-	0.5 mL/L
Coconut water	-	-	-	-	100 mL/L	-	-
IAA	-	-	-	-	-	0.5 mg/L	-
BAP	-	-	-	-	-	0.3 mg/L	-
NAA	-	-	-	-	-	-	0.05 mg/L

Table S2 Composition of the nutrient solutions used to prepare the media for rice transformation. All concentrations are shown in g/L.

	Solution composition																				
	KNO_3	$(NH_4)SO_4$	KH_2PO_4	$MgSO_4 \cdot 7H_2O$	$CaCl_2 \cdot 2H_2O$	Myo-inositol	Thiamine HCl	Nicotinic acid	Pyridoxine HCl	$MnSO_4 \cdot H_2O$	KI	H_3BO_3	$ZnSO_4 \cdot 7H_2O$	$CuSO_4 \cdot 5H_2O$	$Na_2MoO_4 \cdot 2H_2O$	$CoCl_2 \cdot 6H_2O$	NH_4NO_3	$FeSO_4 \cdot 7H_2O$	$Na_2EDTA \cdot 2H_2O$	FeNaEDTA	$NaH_2PO_4 \cdot H_2O$
N6 Macro I	28.3	4.63	4	1.85	-	-	-	-	-	-	-	-	-	-	-	-	-	-	-	-	-
N6 Macro II	-	-	-	-	1.66	-	-	-	-	-	-	-	-	-	-	-	-	-	-	-	-
R2 Macro I	40	3.3	-	2.46	-	-	-	-	-	-	-	-	-	-	-	-	-	-	-	-	3.12
R2 Macro II	-	-	-	-	1.46	-	-	-	-	-	-	-	-	-	-	-	-	-	-	-	-
MS Macro I	19	-	1.7	3.7	-	-	-	-	-	-	-	-	-	-	-	-	16.5	-	-	-	-
MS Macro II	-	-	-	-	4.4	-	-	-	-	-	-	-	-	-	-	-	-	-	-	-	-
B5 Vitamins	-	-	-	-	-	10	1	0.1	0.1	-	-	-	-	-	-	-	-	-	-	-	-
R2 Vitamins	-	-	-	-	-	-	0.04	-	-	-	-	-	-	-	-	-	-	-	-	-	-
LS Vitamins	-	-	-	-	-	10	0.04	-	-	-	-	-	-	-	-	-	-	-	-	-	-
R2 FeNaEDTA	-	-	-	-	-	-	-	-	-	-	-	-	-	-	-	-	-	1.25	0.177	-	-
MS FeNaEDTA	-	-	-	-	-	-	-	-	-	-	-	-	-	-	-	-	-	-	-	3.67	-
B5 Micro	-	-	-	-	-	-	-	-	-	10	0.75	3	2	0.039	0.25	0.025	-	-	-	-	-
R2 Micro	-	-	-	-	-	-	-	-	-	1.6	-	2.83	2.2	0.195	0.125	-	-	-	-	-	-
MS Micro	-	-	-	-	-	-	-	-	-	16.9	0.83	6.2	8.6	0.025	0.25	0.025	-	-	-	-	-

Table S3 CRISPR/Cas9-induced mutations in *ospif* single and double mutant lines. A Single-guide RNA (SgRNA) sequence containing a 20-nucleotide targeting sequence (crRNA) (column 2) was custom-designed for each *OsPIF* gene of interest (column 1) and the proto-spacer adjacent (PAM) motifs at the 3' of each DNA target sequence were also identified (column 3). The genomic DNA of WT plants and T0 generation transformants was amplified and the PCR products were sequenced by Sanger sequencing to identify CRISPR/Cas9-induced insertions and deletions (InDels). The mutations were then reconfirmed (column 5) by Sanger sequencing of Cas9 cassette-free homozygous mutant plants of descendant generations (column 4) obtained through segregation in.

Target gene	SgRNA targeting sequence (5' → 3')	PAM (5' → 3')	Plant line	InDels
OsPIF11	AGGTGCACAACCTCTCCGAG	AGG	*ospif11.1*	-7/-7
	ATCATCCTGCTCTGGAACG	CGG	*ospif11.2*	+1/+1
			ospif11.3	-671/-671
OsPIF12	AAAGACTTGCAAGGGCGACG	CGG	*ospif12.1*	-1/-1
			ospif12.2	-59/-59
			ospif12.3	+1/+1
OsPIF13	ACTCATACCTCATTGCAACA	AGG	*ospif13.1*	+1/+1
			ospif13.2	+1/+1
			ospif13.3	-1/-1
OsPIF14	ACCGCCATCCGCGAACCACG	CGG	*ospif14.1*	-37/-37
			ospif14.2	-4/-4
			ospif14.3	-1/-1
OsPIF15	ACTCATTCCCAACTGCAACA	AGG	*ospif15.1*	-7/-7
			ospif15.2	-4/-4
			ospif15.3	+1/+1
OsPIF16	ACAACAACCAGTCCGCCGAG	TGG	*ospif16.1*	-1/-1
			ospif16.2	-4/-4
			ospif16.3	-20/-20
OsPIF8	GTTGAGCAGCAGGCCATGCG	AGG	*ospif8.1*	-1/-1
			ospif8.2	+1/+1
			ospif8.2	-1/-1
OsPIF15	GTGATGATGACACCGTTCCG	TGG	*ospif15 ospi16.1*	-7/-7; +1/+1
OsPIF16	GCTCTTCTCCGACCAGAGGA	TGG	*ospif15 ospi16.2*	-1/-1; +1/+1
			ospif15 ospi16.3	-1/-1; +1/+1